STRESS RESPONSE AND HYPOTHETICAL GENES IN *DESULFOVIBRIO VULGARIS* HILDENBOROUGH

A Thesis

presented to

The Faculty of the Graduate School

University of Missouri-Columbia

In Partial Fulfillment

of the Requirements for the Degree of

Master of Science

---

by

Elliott C. Drury

Dr. Judy D. Wall, thesis supervisor

DECEMBER 2008

The undersigned, appointed by the dean of the Graduate School, have examined the Thesis entitled

STRESS RESPONSE AND HYPOTHETICAL GENES IN *DESULFOVIBRIO VULGARIS* HILDENBOROUGH

presented by Elliott C. Drury,

a candidate for the degree of master of science,

and hereby certify that, in their opinion, it is worthy of acceptance.

Professor Judy Wall

Professor Mark McIntosh

Professor Michael Calcutt

ACKNOWLEDGEMENTS

First and foremost, I would like to thank my mentor, Dr. Judy Wall. She has had a seemingly infinite amount of patience with me. I am honored to graduate under her tutelage and will treasure my time I have spent at Mizzou.

I also appreciate my committee members, Dr. Mark McIntosh and Dr. Michael Calcutt, who have displayed the same patience and had faith throughout the process.

I would also like to give a shout to all the lab members that have helped me out and taken me under their wing from when I was just a rube. Barbara Giles, Bill 'MixMaster' Yen, Kelly Bender, Dwayne Elias, Grant Zane, Bret Emo, Ray Payne, and Chris Hemme.

All my other coworkers that I have given me many experiences, made some of the rotten days bearable, and able to share a joke with: Jarrod Robertson, Tom Juba, Leena Patarkine, Suzanne Miller, and Isaac Hilton.

And, all the undergraduates that have given me a window back to the beginning stages of science and that I may or may not have taught something to: Matt Shirley, Matt Begeman, Dan Hess, Kate Hart, and Marielis Torres.

Finally, a rebel yell to my friends and sometimes scientists that have always had an ear for me and shared a drink with in success and defeat: Adam 'Pirate' Perkins, J.C. Hardaway, Travis Baughan, Jason 'der' Furrer, Tristan Coady, Steve 'este ban' Smith, and Dr. C.A.

ABSTRACT

STRESS RESPONSE AND HYPOTHETICAL GENES IN *DESULFOVIBRIO VULGARIS* HILDENBOROUGH

Elliott C. Drury

Dr. Judy D. Wall, Thesis Advisor

The sulfate-reducing bacteria (SRB) have a significant impact on the environment and the economy, necessitating further investigation of their physiology to harness their positive attributes and to minimize the damaging byproducts. Through the use of *in vitro* and *in silico* experiments, I have examined some of the metabolic pathways of *Desulfovibrio vulgaris* Hildenborough. The information obtained may contribute to an application of the SRB, *D. vulgaris* in particular, as an effective and economical means of bioremediation and also may play a role in controlling their activity in corrosion of metals and concrete.

During my work on this project, I have developed software tools to expedite the creation of targeted deletion mutants through marker exchange, protein tagging, and to identify the insertion sites of randomly integrated transposons. A substantial amount of microarray data from stressed cultures has been generated by our collaborators that I have analyzed for trends across the experimental conditions. My analysis has yielded new insights to the general and specific stress response systems of *D. vulgaris*. An interesting subset of data, the massive subset of hypothetical genes, offers many tantalizing opportunities for further study with the hints revealed by my analysis. Evidence for the

translation of hypothetical genes, revised annotations of the functional descriptions, and clustering according to gene activation was compiled and used to assist in clarification of the role of some of the hypothetical genes identified within the genome sequence. Finally, physiological characterization of select deletion mutants that I constructed has also revealed interesting involvement of the specific gene products in the stress responses.

The tools that have been developed and the studies undertaken have yielded immediate results that have increased the knowledge base of the SRB. In addition, further questions became evident whose answers will hopefully lead to critical breakthroughs to reach the ultimate goal of a natural bioremediation tool.

LIST OF TABLES

LIST OF FIGURES

TABLE OF CONTENTS

Chapter 1

INTRODUCTION

1.1 Sulfate-Reducing Bacteria

The sulfate-reducing bacteria (SRB) play an important, but not yet fully understood, role in nature which has a significant impact on the environment and the economy. The SRB are primarily defined by their ability to utilize sulfate, $SO_4^{=}$, as their terminal electron receptor (Postgate, 1979). This metabolic capability is known as dissimilatory sulfate reduction (Postgate, 1979).

There are five distinct categories of sulfate reducers (Barton and Hamilton, 2007), with the first group, mesophilic δ-proteobacteria, containing the strains that will be most discussed throughout this document.

Between the groups there are more differences than obvious differences gathered from the naming conventions, such as: membrane traits, environmental niches, and evolutionary relationships. These groups differ in doubling rates (Nanninga and Gottschal, 1987; Macy *et al.*, 2000; Pfennig *et al.*, 1989), diversity of terminal electron acceptors (Lovley *et al,.* 1993; Lovley and Phillips, 1992; Lovley and Phillips, 1994), growth substrate capabilities (Ollivier *et al.*, 1988; Parshina *et al.*, 2005; Tanimoto and Bak, 1994), oxygen resistance (Sass *et al.,* 1997) and respiration byproduct production (Brandis-Heap *et al.,* 1983).

Interaction between the SRB and a wide range of other organisms occurs in both symbiotic and competitive relationships. Regions previously considered oxic have been shown to support SRB growth when a protective anaerobic layer is present through natural sediment layers (Jorgensen, 1977) or bacterial interfaces and biofilms (Schramm

et al., 1999). When growing in a niche with excess sulfate, the SRB are also known to compete with the methanogens for other necessary substrates, such as hydrogen and acetate (Stams *et al.*, 2003). Few studies have compared SRB growth patterns in sulfate limitation with those of other organisms (Stolyar *et al.,* 2007 and Laanbroek *et al.*, 1984). This characteristic will be discussed throughout this chapter, both in general across the SRB and *Desulfovibrio* in particular. The defining property of sulfate respiration allows these bacteria to colonize sulfate-rich habitats restricted for other bacteria.

1.2 Sulfate Reduction

The SRB are ever present in the environment. They can be found in locations as diverse as fresh (Vladar *et al*., 2008) or salt water (Ravenschlag *et al*., 2000), oil fields (Nilsen *et al*., 1996), and even the human intestine (Moore *et al*., 1976). The common link between these conditions is sulfate availability.

Sulfate reduction is the process by which the transfer of electrons from donor substrates to oxidized sulfur compounds allows the generation of ATP (Fig. 1.2.1). This pathway is described for *D. vulgaris* in Hansen, 1994. The SRB are uniquely capable of reducing sulfate to sulfide for a gross production of three ATP, although it takes the equivalent of two ATP to activate sulfate to Adenosine-PhosphoSulfate (Sperling *et al.*, 1998) in preparation for reduction (Badziong and Thauer, 1978). Both sulfite and thiosulfate can also serve as respiratory substrates for these bacteria. There has been some argument whether thiosulfate is reduced to sulfite and sulfide and then generating energy via the sulfite reduction step, or if the first step in thiosulfate utilization is dismutation to sulfate and sulfide followed by normal sulfate activation and reduction (Bak and Pfennig, 1987 and Bottcher *et al.*, 2005).

Figure 1.2.1 Sulfate reduction pathway (reproduced from Wall lab, unpublished). The various states of the reduced sulfur compounds are colored in green. The flow and energetic components are black. Sulfate requires two ATP equivalents for activation that sulfite does not require to be a terminal electron acceptor, but sulfate allows eight electrons to be removed, compared to six for sulfite. There is a gross yield of 3 ATP for the reduction of sulfate to sulfide (Badziong and Thauer, 1978).

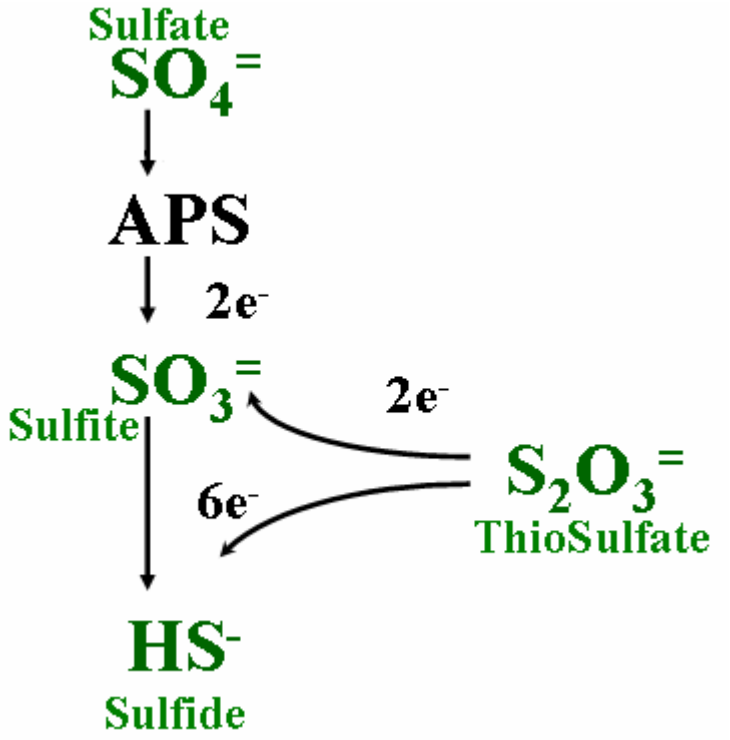
Sulfate
$SO_4^=$
APS
$2e^-$
$SO_3^=$
Sulfite
$2e^-$
$6e^-$
$S_2O_3^=$
ThioSulfate
HS^-
Sulfide

There is a wide range of electron donors that the SRB are capable of using. The genus *Desulfovibrio* has a more limited array of substrates that include lactate, formate, hydrogen and pyruvate (Muyzer and Stams, 2008). A few *Desulfovibrio* species can utilize sugars (Sass *et al.,* 2002), amino acids (Stams *et al.,* 1985), methanol (Nazina *et al.,* 1987), and carbon monoxide (Parshina *et al.,* 2005). Macromolecular substrates like starch, proteins, and nucleic acids are incapable of being reduced by the SRB without a codependent relationship with other bacteria that can break down these substrates (Muyzer and Stams, 2008).

The ability to respire sulfate persists across all SRB, but some genera are more easily cultured and, therefore, have been studied in greater detail. Strains of those genera have a more mature knowledge base, more advanced tool sets and have been characterized more extensively. Several *Desulfovibrio* species are genetically accessible, thereby allowing the use of many vectors that have been developed to generate mutants or look for genetic expression. Thus these model organisms are more attractive for laboratory research.

1.3 Benefits and Concerns

The past few years has brought much research attention to the SRB for their potential as bioremediators of chemically contaminated sites. In addition, the metal corrosion correlated with their growth in the environment has also brought attention to these bacteria, albeit of a more negative nature, because of the damage to physical structures and economic losses.

During the Cold War enrichment of uranium was required for the construction of nuclear weapons and lead to significant quantities of chemical waste being buried in

metal canisters (http://www.osti.gov/energycitations/product.biblio.jsp?osti_id=897388). Over time, these metal canisters began to leak causing uranium to seep into the soil and ultimately into groundwater. Uranium is harmful to all forms of life and its effects are biomagnified through the food chain (Durbin et al., 1997). Biomagnification occurs as a toxic chemical stored in the tissue of lower life forms is consumed by organisms higher up the chain resulting in greater quantities of toxic chemicals accumulated in the higher life forms.

Previous efforts to remove contaminating uranium focused on soil excavation (Program, 2003). This procedure was carried out by removing contaminated soil, detoxifying or washing the mass at an offsite location, and then returning the "cleaned" soil to the original site. This invasive and disruptive method was not cost effective and also caused lasting ecological damage at the sites of remediation. It was proposed to use a biological approach to detoxify the uranium infused sites (Program, 2003). Since the SRB are capable of using uranium as a terminal electron acceptor and are naturally widespread in soils, these bacteria were a logical choice to examine a microbial bioremediation process.

The SRB reduce Uranium(VI) creating Uranium(IV) (Lovely, 1993). U(IV) is an insoluble mineral UO_2, uraninite, that is biologically unavailable and no longer an ecological threat. An example of this is shown in Figure 1.3.1 where *D. desulfuricans* G20 has been shown to generate uraninite. This mineral form has been confirmed by synchrotron analysis of the redox state (Payne, 2002).

1.3.1 Uranium reduction by *Desulfovibrio desulfuricans* G20. The tubes contain *D. desulfuricans* G20, the left has been heat killed and the right contains live cells. The medium is 5 ml of 30 mM sodium bicarbonate buffer at pH 7.0 with 10 mM lactate and 1 mM U(VI). Anaerobic incubation at 31ºC showed reduction of U(VI) to U(IV), a black precipitate – uraninite, only in the presence of live *D. desulfuricans* G20 cells. (Figure reproduced from Payne, 2005).

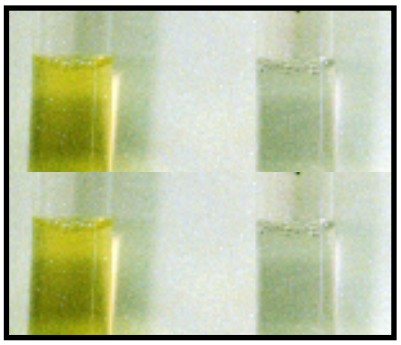

U(VI) (Soluble) → U(IV) (ppt)

+ 2 e^-

Not all the metabolic activities of the SRB are considered to be beneficial. In fact these bacteria have historically come to our attention because they are considered to be the causative agent of anaerobic metal corrosion (Postgate, 1984). This biocorrosion of metals has been proposed to occur through the mechanism of cathodic depolarization (Kuhr and Vulgt, 1934) (Fig. 1.3.2). The removal of electrons from elemental iron, either directly or through a hydrogen intermediate, ionizes the metal causing it to become soluble in aqueous environments. This phenomenon of solubilizing metal ions causes pitting corrosion. This is especially troublesome in the petroleum industry where oil wells and pipelines are both clogged with microbial biomass and corroded resulting in leakage of oil into the environment (Hamilton, 1985). In addition to this, the SRB "sour" oil products with sulfide, the end product of sulfate respiration (Odom, 1993). This contaminated fuel requires a more involved refinement process and generates higher levels of pollution.

Concrete sewer lines are also susceptible to biocorrosion by the SRBs. The hydrogen sulfide gas produced by the SRB in anoxic biofilm environments interacts with sulfide-oxidizing bacteria residing in oxygen rich condensates at the top of the pipes. These bacteria generate sulfuric acid as a result of their respiratory activity and the acid destroys the concrete (Odom, 1985). This reaction and corrosive damages are most common in warm weather regions with minimal elevation changes throughout the sewer system allowing optimal microbial growth.

Fig 1.3.2 Cathodic depolarization of iron (reproduced from Miller, 2005). Metal electrons reduce water to elemental hydrogen. At this point the metal ions are solubilized and the surface becomes pitted.

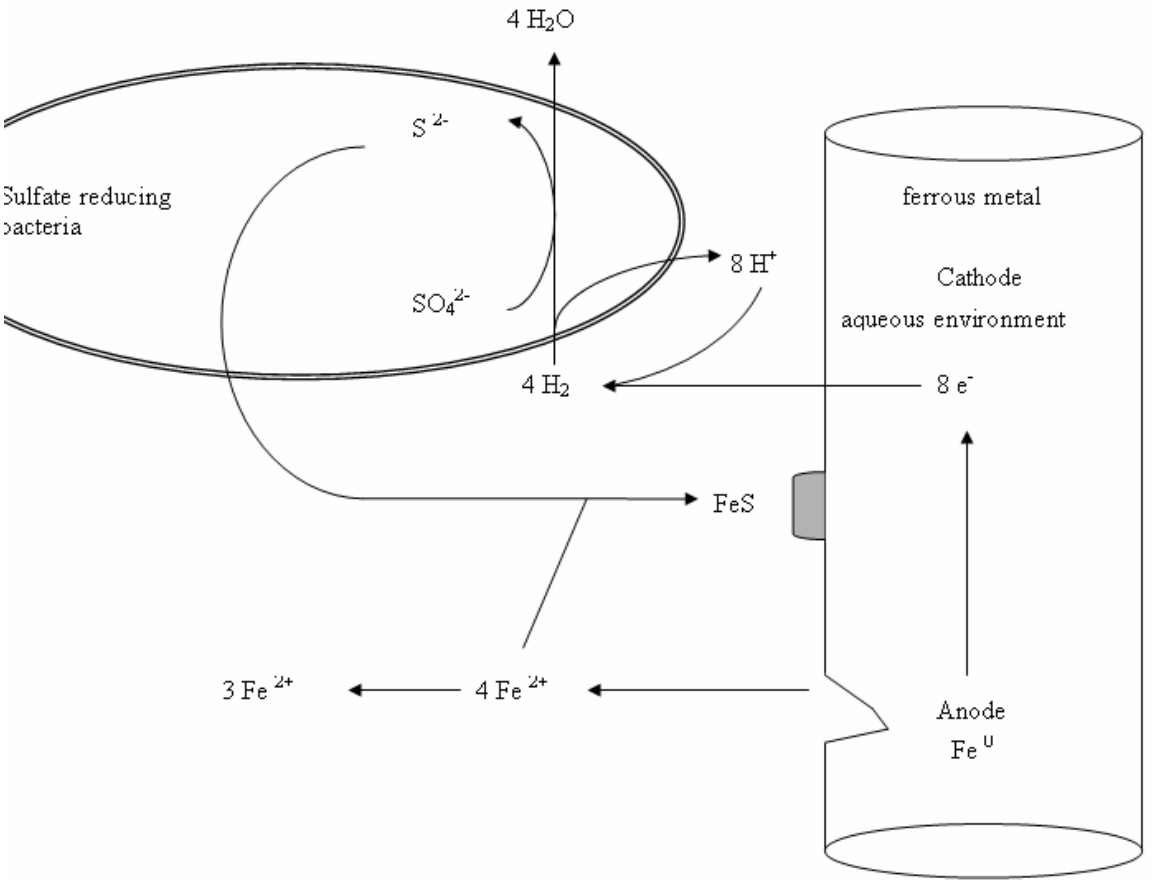
4 H2O
S 2-
Sulfate reducing
bacteria
SO4 2-
8 H+
ferrous metal
Cathode
aqueous environment
4 H2
8 e-
FeS
3 Fe 2+
4 Fe 2+
Anode
Fe 0

1.4 *Desulfovibrio*

Desulfovibrio are Gram-negative, strict anaerobes that are incomplete oxidizers of organic compounds (Beijerinck, 1895). The two specific strains used in the following studies are *Desulfovibrio vulgaris* Hildenborough and *Desulfovibrio desulfuricans* G20. *D. vulgaris* Hildenborough was initially isolated from Wealden Clay outside of Hildenborough, Kent in the United Kingdom in 1946 (Postgate, 1984). *D. desulfuricans* G20 was originally cultured from an oil well in Ventura County, CA in 1987 (Weimer *et al.*, 1988). These two *Desulfovibrio* species are used in the Wall lab because of their ease of culturing, resources available for their investigation, and the amount of previous work invested into these organisms. These strains have a reasonable doubling time of approximately four hours (Nanninga and Gottschal, 1987) compared with other SRB that have doubling times at least twice as long (Macy *et al.*, 2000 and Pfennig *et al.*, 1989). They are also genetically accessible with shuttle vectors used for insertion of foreign sequences and selectable markers identified. Possibly one of the most important resources is that the genomic sequences of these organisms are publicly available (Heidelberg et al., 2004 and www.jgi.doe.gov).

1.5 Respiration

Members of the *Desulfovibrio* genus are capable of using substrates other than sulfate and sulfite as terminal electron acceptors. Substrates included in this category are iron (Park *et al.*, 2007), uranium (Payne, 2005), chromium (Lovley and Phillips, 1994), mercury (Barton and Hamilton, 2007), and selenate (Tucker *et al.,* 1998). Although these substrates are reduced, this process is not connected to ATP generation. Hence, *Desulfovibrio* is not capable of growth while transferring electrons to these acceptors.

Electron transfer to these substrates has far reaching effects for the application of these bacteria to environmental problems.

The *Desulfovibrio* genus is a group of incomplete oxidizers meaning that acetate is the final byproduct of degradation of electron donor and carbon substrates (Brandis-Heap *et al.,* 1983 and Steger *et al.,* 2002). Also, *Desulfovibrio* is capable of growth by fermentation, using pyruvate as an electron donor and using elemental hydrogen as an acceptor (Muyzer and Stams, 2008). Perhaps the most dramatic increase in understanding these bacteria has derived from the availability of the genome sequences of a small number of these bacteria (microbesonline.org). Sequence information has lead to directed research and results that would otherwise not have been possible; for example, an understanding of the role of temperate bacteriophage in the evolution of the bacterium.

1.6 Genome

Approximately a dozen SRB genomes have been sequenced or are currently being sequenced (Klenk *et al.*, 1997; Rabus *et al.*, 2004; Muyzer and Stams, 2008). Among these are five bacteria in the *Desulfovibrio* genus, including the two primarily used in these studies, *D. vulgaris* Hildenborough and *D. desulfuricans* G20.

The *D. vulgaris* Hildenborough sequence was published in 2004 (Heidelberg et al., 2004). The genome consists of a main chromosome and a native plasmid, pDV1, consisting of 3.57 Mb and 203 kb, respectively. pDV1 is not essential for survival of the organism and a strain lacking this plasmid has a distinct physiological phenotype of slower growth rate and impaired nitrogen fixation compared to the wild type strain (Clark *et al.*, 2007). The conditions which naturally cure *D. vulgaris* Hildenborough of pDV1 are currently unknown. There are 3527 and 147 predicted gene coding sequences across

the chromosome and native plasmid which have GC contents of 63.1% and 65.7%, respectively.

Of the predicted 3527 predicted genes, 34% are annotated as hypothetical or conserved hypothetical genes. Hypothetical genes are ORFs that are predicted by computer algorithms and bear homology to no other annotated genes. Conserved hypothetical genes are predicted in the same fashion, but share homology with putative genes from other closely related bacteria. Of the *D. vulgaris* genes, 280 have been initially annotated as conserved hypothetical genes and share homology with conserved hypothetical genes in *D. desulfuricans* G20.

The *D. desulfuricans* G20 (www.jgi.doe.gov) sequence consists of a single chromosome of 3291 genes with a 57.8% GC content. Despite sharing homology of 280 conserved hypothetical genes with *D. vulgaris*, these two bacteria are different in aspects of their physiology concerning oxygen resistance and cytochrome *c* production (Wall lab, unpublished). Initial computational analysis and characterizations of these genomes have been published (Rodinov *et al.*, 2004). These developments stemming from advances in sequencing technology have provided the impetus for segments of the research presented here because of the availability of full genome sequences. The advances in sequencing technologies have enabled the prediction of operons, regulons and the development of "omics" tools.

1.7 Genetic Techniques

An ever increasing repertoire of genetic manipulation techniques have allowed the knowledge base of the SRB, specifically the *Desulfovibrio*, to advance. A useful set of shuttle vectors was developed with a small cryptic plasmid, pBG1 (Rousset *et al*., 1993).

These vectors paved the way for transformation of *Desulfovibrio* by electroporation. Multiple methods to create mutants have evolved from this original research. Targeted genetic deletions were accomplished by marker exchange induced through a suicide plasmid (Giaver *et al*., 2002). Mutant libraries were constructed with integration of a transposon carrying plasmid (Larson et al., 2002). Translational gene fusions were created via homologous recombination of a suicide plasmid vectors to view protein localization and ascertain protein/protein interactions (Wall lab, unpublished). My research has also used these genetic tools to create deletions. Software utilities were developed by me to optimize and analyze these genetic manipulation techniques and the mutants they created.

Microarray technology advancements have allowed for quantitative gene regulation measurements. Full genome transcript analysis was performed by using RNA normalized to genomic DNA (Mukhopadhyay *et al*., 2006). This method allowed for every gene to have quantitative, as well as qualitative, measurements. This new microarray technique was applied to cells grown in media with sub-lethal quantities of common environmental stressors or limitations or excesses of essential growth substrates. These targeted treatments produced better insight into genome regulation and metabolic pathway connectivity. The ability to view the entire genomic response simultaneously lead to breakthroughs in the annotation of all expressed hypothetical genes. These response data were compiled for many cellular treatments and, upon evaluation, suggested potential roles for the hypothetical genes that required further exploration.

1.8 Specific Aims

The purpose of this study was to investigate metabolic pathways in *D. vulgaris.* Computational analysis of stress response microarray treatments was performed to ascertain novel pathways and gene interactions. This analysis lead to functional descriptions annotated for the hypothetical genes, approximately 33% of the genome. Along with the computational analysis, a variety of software utilities were developed to expedite continued *in vivo* experiments stemming from the aforementioned results. Deletion mutants were created in *D. vulgaris* to assess physiological hypotheses derived from the computational analysis. Genes selected for deletion had putative roles in general stress response, chromium resistance, and ion transport. These deletion mutants were the focus of growth experiments with the aim to elucidate growth impairment, substrate specificity and toxin resistance.

Chapter 2

MATERIALS AND METHODS

2.1 Media

To ensure that data from multiple experiments could be compared, a single defined medium was used for all environmental stress experiments generating transcriptomic and proteomic data. LS4D (60 μM total iron) consisted of 60 mM sodium lactate, 50 mM Na_2SO_4, 8.0 mM $MgCl_2$, 20 mM NH_4Cl, 2.2 mM K_2HPO_4, 0.6 mM $CaCl_2$, 30 mM PIPES [piperazine-N,N'-bis(2-ethanesulfonic acid)], 12.5 ml trace mineral solution per liter (Brandis and Thauer, 1981), NaOH to a pH of 7.2, and 1.0 ml Thauer's vitamin solution per liter (Brandis and Thauer, 1981). One tenth gram of yeast extract was added per 100 ml of LS4D for non-defined medium, designated LS4.

For physiological experiments of mutants to determine substrate utilization and growth kinetics, a medium based on Tris buffer was designed to decrease the precipitate in the medium. Yen45 (30 μM total iron) consisted of 8.0 mM $MgCl_2$, 20 mM NH_4Cl, 2 mM phosphate (K_2HPO_4/NaH_2PO_4, pH 7.4), 0.6 mM $CaCl_2$, 30 mM Tris-HCl (pH 7.4), and, per liter, 2 ml modified trace mineral solution (modified by omission of nitrilotriacetic acid and $FeCl_2$), 0.24 ml iron solution (125 mM $FeCl_2$, 250 mM EDTA, pH 7.3), 20 ml sterile 1 M $NaHCO_3$ (added after autoclaving), and 1.0 ml sterile Thauer's vitamin solution per liter (Brandis and Thauer, 1981).

As the reductant for both media, 5 ml of an anaerobic titanium citrate solution per liter was used. This solution contained 20% (wt/vol) titanium(III) chloride, 0.2 M sodium citrate, and 8.0% (wt/vol) sodium carbonate.

For plating, LS4D medium was supplemented with 0.2% (wt/vol) yeast extract, 1.5% (wt/vol) agar, and 1.2 mM thioglycolate.

Liquid Yen45 medium was used for all growth curve experiments (unless otherwise explicitly noted). Growth was measured by 'OD_{600}', the optical density measured at 600 nm. All LS4D and Yen45 variations were adjusted sterilely to a pH of 7.2 after addition of all components.

Standard concentrations for electron donors and acceptors are listed in Table 2.1.1 and were used in Yen45-based media. These combinations will be designated as 'donor / acceptor' in all future references of this document.

LC medium for *Escherichia coli* is composed of 10 g tryptone, 5 g yeast extract, and 5 g NaCl, and solidified, when desired, with 15 g agar per liter of medium. LC was adjusted to a pH of 7.0.

2.2 Marker Exchange Mutagenesis

The deletion cassette methodology was adapted from Giaever et al. in 2002 that was used to generate deletions in *Saccharomyces cerevisiae*. Primer listing, sequence analysis, plasmid designations, Southern blot analysis, *E. coli* transformation, and genomic DNA preparations are included below in unique subchapters. The general procedure is described in the paragraphs following.

The strategy for deleting a gene from the bacterium was to clone approximately 1 kb of sequence upstream and approximately 1 kb of sequence downstream of the target gene on either side of an antibiotic resistance cassette (in this case, containing the kanamycin resistance gene from Tn*5* encoding neomycin phosphotransferase).

Table 2.1.1 Concentrations of various electron donors and acceptors used.

DONOR		ACCEPTOR	
Lactate	60 mM	Na_2SO_4 (sulfate)	30 mM
Pyruvate	60 mM	Na_2SO_3 (sulfite)	40 mM
Formate / Acetate	60 mM / 60 mM	$Na_2S_2O_3$ (thiosulfate)	40 mM
EtOH (ethanol)	60 mM		

The three segments would be amplified by PCR and then spliced by overlap extension (SOEing) through PCR reactions (Warrens *et al*., 1997). This mutagenic cassette (Fig. 2.2.1) would then be introduced into the cell where a double recombination event would replace the target gene with the drug resistance gene. The antibiotic resistance cassette contained a sequence common to all deletion mutations constructed in the Wall lab and a barcode unique to each target gene on each end. Both the common sequences (26 bp each) and the barcodes (20 bp each) were introduced into the kanamycin resistance cassette by inclusion in the primers used for amplification of the drug resistance gene. The barcodes would allow differentiation among deletion isolates when grown simultaneously (Giaever et al, 2002).

The drug resistance cassette, upstream and downstream regions were PCR-amplified with the Herculase polymerase mixture (Stratagene, La Jolla, CA) and joined using SOEing PCR (Warrens *et al*., 1997). The resulting product (generically called "PCR4," Fig 2.2.1) was separated on a 0.8% (wt/vol) agarose gel, the appropriate band excised and cleaned with the Wizard SV Gel and PCR Clean-up system (Promega, Madison, WI). PCR4 was then captured in the cloning vector pCR8-TOPO encoding spectomycin resistance (Invitrogen, Carlsbad, CA), generating plasmid pMO### (numbered according to the targeted gene), and transformed into competent *E. coli* TOP10 cells (Invitrogen, Carlsbad, CA). The transformed cells were allowed to recover for 1h at 37^{o}C and plated onto solidified LC medium with 50 µg kanamycin/ml (Fisher, Pittsburgh, PA). From the LC plates, the putative transformant colonies were inoculated into 5 ml of LC medium containing 50 µg kanamycin/ml and grown aerobically overnight at 37^{o}C.

Figure 2.2.1 Diagram of primers used to create PCR4 and sequence the vector and putative mutants (listed in Table 2.8.3).

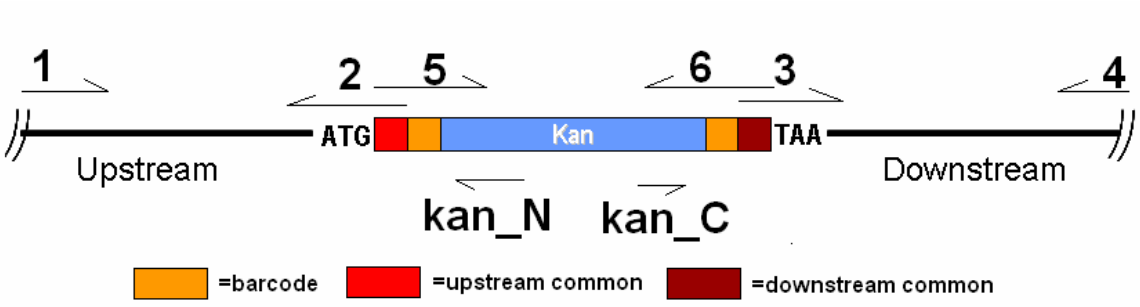
1
2
5
6
3
4
ATG
Kan
TAA
Upstream
Downstream
kan_N
kan_C
=barcode
=upstream common
=downstream common

The mutagenic plasmid was isolated from the kanamycin and spectinomycin resistant *E. coli* transformants by use of the Qiaprep Spin Miniprep kit (Qiagen, Valencia, CA), sequenced in both directions to verify correct upstream, downstream, barcode and common sequences, and electroporated (Chapter 2.8) into competent *D. vulgaris*. Electroporated *D. vulgaris* cells were allowed to recover overnight in 1 ml of lactate/sulfite medium and plated in molten LS4 medium containing 400 µg G418 (Geneticin)/ml (RPI corp., Mt. Prospect, IL), the most effective antibiotic selector of kanamycin resistance in *D. vulgaris*. Three volumes (10 µl, 100 µl, and 890 µl) of the putative transformants were plated to increase the likelihood that single colonies could be obtained. Growth was observed after 3-5 days of anaerobic incubation at 30^{o}C. Of the colonies which were resistant to G418, five were inoculated into 0.5ml lactate/sulfite medium with 400 µg G418/ml and 0.1% yeast extract (wt/vol) and grown overnight at 30^{o}C. On the following day, three of the isolates that grew were subcultured into 5 ml of the same medium and grown again overnight at 30^{o}C to expand the culture. On the next day, 1.5 ml of culture was used for preparation of genomic DNA using the Wizard Genomic DNA purification kit (Promega, Madison, WI) and 3.5 ml of culture was used to make freezer stocks (prepared by the addition of sterile glycerol, final concentration of 10% (vol/vol), 0.75 ml aliquoted into cryogen tubes, and stored at -80^{o}C).

2.3 Southern Blot Analysis

For Southern confirmation of the marker-exchange mutagenesis, genomic DNAs of putative mutants and wild-type *D. vulgaris* (4 µg of each) were digested with 10 units of a restriction endonuclease according to the instructions of the manufacturer (NEB, Beverly, MA) for 4 h and separated by electrophoresis on two different 0.8% (wt/vol)

agarose gels at 85V for 1.5 h. The restriction endonuclease was selected to not cut the targeted gene or the kanamycin antibiotic resistance cassette. The DNA was then transferred onto a Zeta-probe membrane in 0.5 M NaOH overnight through capillary diffusion. The DNA was cross-linked to the membrane with UV irradiation of 120 mJ/cm^2 delivered over 20 sec. The membranes were incubated in hybridization solution (0.5 M NaH_2PO_4, 7.5% (wt/vol) SDS, 1 mM EDTA) for 30 min at 65^oC. One membrane was probed with the gene deleted and the second membrane was probed for the kanamycin resistance marker. The probes were created using the Prime-It II kit (Stratagene, La Jolla, CA). After overnight hybridization to the probe, the membranes were washed once with wash solution 1 (2 x SSC and 0.1% (wt/vol) SDS) for 30 min at 65^oC and once with wash solution 2 (0.1 x SSC and 0.1% (wt/vol) SDS) for 30 min at 65^oC. The membrane was then exposed to CL-X Posure Film (Pierce, Rockford, IL) overnight at -80^oC and developed. DNA fragment sizes were determined by comparison with the best-fit line of the distance of migration plotted against the log of the length in nucleotides of the members of the 1 kb DNA ladder standard (NEB, Beverly, MA).

2.4 Transposon Insertion

Tn*5*-RL27 transposon (Larson et al., 2002) mutagenesis occurs by a mechanism in which a segment of DNA (transposon) encoded in a plasmid is inserted into genomic DNA (the target) by a conservative cut-and-paste mechanism. pRL27, that encodes a mini-Tn*5* transposon, Tn*5* transposase, and a kanamycin resistance gene (Larson et al., 2002), was used to transform *D. vulgaris* Hildenborough by electroporation. Location of the insertion site of the transposon should be able to be determined by direct sequencing from the chromosome. This technique has not been successful, possibly due to

competition of inexact binding sites in genomic DNA for the sequencing primers (Barbara Giles and Matthew Shirley, unpublished). A higher concentration of transposon insertion sites was determined to be needed to yield quality sequencing results.

A nested PCR method that allowed enrichment of the desired transposon insertion site was successful (Chun et al, 1997). This nested semi-random PCR methodology creates a high concentration of the DNA flanking the transposon sequence that facilitates direct, quality sequences of the amplified product to be obtained. This process and the use of a custom software tool described in Chapter 6.3 made locating Tn*5*-RL27 transposon insertion sites as easy as PCR.

The electroporation, plating, and colony isolation techniques used during transformation were identical to those used during marker exchange mutagenesis described in Chapter 2.2.

2.5 Microarrays

The RNA isolation techniques, kits used, and other specific products were performed by the Hazen and Zhou laboratories and detailed in other papers (Chhabra *et al.*, 2006; He *et al.*, 2006). These procedures are quoted from Mukhopadhyay et al. (2006) below to allow readers to understand the data used for stress response comparisons and exploring functions for the hypothetical genes in *D. vulgaris*. Because these experiments were not conducted by me and not in the Wall lab, I have not altered any verbiage.

> "Culture maintenance. *D. vulgaris* Hildenborough (ATCC 29579) was obtained from the American Type Culture Collection (Manassas, VA). For all experiments and culture maintenance we used a defined lactate sulfate medium (LS4D medium) based on Postgate's medium C (Postgate, 1984). . . . and 5 ml of titanium citrate. To prepare titanium citrate, 500 ml of 0.2 M sodium citrate was boiled for 20 min under a continuous stream of

nitrogen to remove dissolved oxygen. While the preparation was hot, 37.5 ml of 20% (wt/vol) $TiCl_3$ was added along with 100 ml of 8% (wt/vol) Na_2CO_3 under nitrogen. The final mixture was autoclaved and used. Subculturing was minimized by using –80°C *D. vulgaris* stocks as 10% inocula for 100- to 200-ml fresh LS4D medium starter cultures at the mid-log phase of growth (optical density at 600 nm [OD_{600}], 0.3 to 0.4). These cultures were then used as 10% inocula for 1- to 3-liter production cultures. All cultures were grown at 30°C.

MIC. MIC was defined as the stressor concentration that doubled the generation time and/or decreased the overall yield by 50%. Growth curve experiments were conducted in 96-well plates using an OmniLog instrument (Biolog Inc., Hayward, CA), which captured digital optical density images every 15 min for 150 h. Each well was inoculated with 10% mid-log-phase cells, six replicates of each stressor dilution were used, and the plates were placed in an anaerobic atmosphere and sealed in airtight Retain bags (Nasco) before they were placed in the OmniLog. OmniLog measurements were calibrated against *D. vulgaris* cell densities obtained by determining the OD_{600}, using a Biolog plate reader, and determining direct cell counts by the acridine orange direct count method. All growth curves were comparable at 95% confidence intervals for the exponential growth phase. A kinetic plot of *D. vulgaris* growth was used to determine the generation time and cell yield. For NaCl and KCl stress, the MIC for *D. vulgaris* was determined to be 250 mM (in addition to the concentration present in LS4D medium) by testing concentrations ranging from 0 to 5,000 mM. For all experiments in this study, 250 mM NaCl or KCl was added to growth medium to establish stress conditions.

Biomass production. Highly controlled and reproducible conditions were used for simultaneous production of cell cultures for transcriptomics, proteomics, metabolite assay, PLFA, and synchrotron Fourier transform infrared (sFTIR) spectromicroscopy studies. Control and experimental production cultures were prepared in triplicate. Cultures were exposed to stress at the mid-log phase to minimize in-culture variability. NaCl or KCl (250 mM) was added to experimental cultures, and an equivalent volume of sterile distilled water was added to control cultures. The time of stressor addition was defined as zero time, and samples were taken at 30, 60, 120, and 240 min after exposure. The longest time (<5 h) was less than one generation time, so all samples were collected prior to the stationary phase. Samples were chilled to 4°C in <15 s during collection by pulling samples from production cultures through 7 m of capillary tubing immersed in an ice bath using a peristaltic pump. Chilled samples were centrifuged, and pellets were washed with 4°C degassed sterile phosphate-buffered saline and centrifuged again at 6,000 x *g* (10 min, 4°C). The final pellet was flash frozen in liquid N_2 and stored at –80°C. For the production of each biomass sample, the following purity and growth characteristics were recorded: temperature, pH, OD_{600}, acridine orange direct count, sFTIR

spectrum, total protein content, anaerobic colony morphology, absence of aerobic colonies, and PLFA biosignatures.

. . .

Microarray analysis. Oligonucleotide probe design and microarray construction have been described previously (Li, He, and Zhou, 2005). After RNA extraction, purification, and labeling, a reverse transcription reaction was used to generate labeled cDNA probes. Labeled genomic DNA (Cy3) was used as a control and as the common reference to cohybridize with labeled RNA (Cy5) samples for each slide. Each comparison was done in triplicate. Finally, since there were duplicate arrays on a given slide and three biological replicates, there were a total of 18 possible spots for each gene. Hybridized microarray slides were scanned using the ScanArray Express microarray analysis system (Perkin-Elmer, Massachusetts). Spot signals, spot quality, and background fluorescence intensities were quantified with ImaGene, version 5.5 (Biodiscovery Inc., Los Angeles, CA). For raw microarray data see NCBI GEO accession number GSE4447.

Computational. (i) Gene models. Models of The Institute for Genomic Research (NCBI) were used.

(ii) Microarray data analysis. Log expression levels, including global normalization, were first computed for each microarray. Log expression levels obtained from replicate arrays were averaged. Each gene was represented by two spots on each microarray, and spots flagged by the scanning software were excluded. The net signal of each spot was calculated by subtracting the background signal and adding a pseudosignal of 100 to obtain a positive value. For resulting net signals of <50, a value of 50 was used. For each spot, the level of expression was the ratio of the two channels (ratio of mRNA to genomic DNA). For each replicate, the levels were normalized so that the total expression levels for the spots that were present on all replicates were identical. Finally, mean expression levels and standard deviations of each spot were calculated, which required $n > 1$. To estimate differential gene expression in control and treatment conditions, normalized log ratios were used. The log ratio was $\log_2$(treatment) – $\log_2$(control). This log ratio was normalized using LOWESS on the difference versus the sum of the log expression level (Dudoit and Frindlyand, 2002). Sector-based artifacts were observed; therefore, the log ratio was further normalized by subtracting the median of all spots within each sector. Up to this point, data were processed using spots instead of genes to allow sector-based normalization. Finally, the spots for each gene were averaged to obtain a final normalized log ratio. To assess the significance of the normalized log ratio, a *Z* score was calculated by using the following equation, $Z = \log_2$ (treatment / control) / ($(0.25)^{1/2}$ + Σvariance), where 0.25 is a pseudovariance term. Log ratios and *Z* values for all microarray data in this study are listed in a supplemental data file (http://vimss.lbl.gov/SaltStress/). The log ratios and

> *Z* values were used to generate two types of plots, (i) volcano plots and (ii) operon-based estimates of local accuracy. For volcano plots, we plotted the $\log_2$ ratio of all genes versus *Z* . This provided an estimate of the total numbers of significant changers in a microarray comparison and allowed determination of which time showed the most changers (http://vimss.lbl.gov/SaltStress/). For operon-based estimates of local accuracy, each point represented a group of 100 predicted significant changers with similar *Z* scores (the point showed the least significant *Z* value in the set). The estimated accuracy of each group of changers was derived by inspecting other genes in the same operons as these changers (http://vimss.lbl.gov/SaltStress/). For random changers, the transcripts for 50% of these genes should have been regulated in the same direction, and for perfect changers 100% of the genes should have been regulated in the same direction. Members of the operons without a consistent signal across replicates ($Z < 0.5$) were excluded. Even with perfect microarray data, the estimated accuracy was somewhat less than 100% due to errors in operon predictions. Typically, a cutoff *Z* value of >2 provided accurate significant changers."

The microarray technique quoted above is unique compared to a standard microarray that only measures changes in gene expression, as denoted by the blue line in Fig. 2.4.1. This leaves all other genes to be considered as not changing in expression in response to the particular treatment, the yellow and purple lines in Figure 2.4.1. This obviously omits information about the level of expression of all genes. Normalizing the RNA signal to that of genomic DNA using techniques described above allows the relative level of expression to be measured and thus determine the basal level of mRNA abundance. The basal level of expression can be indicated, as high or low, for genes regardless of significant alterations in expression in response to treatments. All transcript determinations for the treatments listed in Table 2.4.1 were normalized to DNA hybridization. For most *D. vulgaris* Hildenborough genes, mRNA expression levels have about 170 data points for cells grown on LS4D medium to an OD_{600} of 0.3 - 0.4 at 30 Cº.

Table 2.4.1 Stress Conditions [A].

[A] Unless otherwise noted, sampling times were initiated at a set at OD_{600}, usually at 0.3 OD_{600} values of 0.3 and 0.8 correlated to exponential and stationary phases, respectively.

[B] For stationary phase gene expression, comparisons of transcripts were with exponential phase cultures and early stationary phase. At nine time points across the growth curve, cells were sampled, RNA was extracted, and comparisons were made with RNA from samples taken at OD_{600} values of 0.3 and 0.8, correlating to early exponential phase and stationary phase, respectively.

[C] The wild type and, separately, the Δ*perR* mutant were challenged with exposure to 1 or 4 mM peroxide. The control samples had an equivalent volume of water added.

[D] All control comparison samples were untreated *D. vulgaris* in LS4D medium at an OD_{600} matching that of the experimental culture at the initiation of treatment. Control time points mirrored those of the treated sample.

Stressor	Concentration / Condition	Sampling Times (minutes) [B]
Cold	8ºC	60, 120, 240
Heat	50ºC	0, 15, 30, 60, 90, 120
Oxygen	0.1 %	0, 30, 60, 120, 240
Alkaline pH	pH 10	0, 30, 60, 120, 240
Acid pH	pH 5.5	0, 30, 60, 120, 240
Nitrite	2.5 mM	0, 30, 60, 90, 150, 240
Nitrate	105 mM	0, 30, 60, 120, 240, 480
Sodium	250 or 500 mM	0, 15, 30, 60, 120, 240
Potassium	250 mM	0, 30, 60, 120, 240
Chromate	0.45 or 0.55 mM	0, 30, 60, 120, 240
Stationary phase [C]		Time points based on OD_{600}
Peroxide [D]	1 or 4 mM H_2O_2	0, 30, 60, 120, 240, 480
CoCulture	Grown with *M. maripaludis*	End point
Strain Comparison	JW801 vs. WT	0, 30, 60, 120, 240
Mutant: Δ*perR*	1 or 4 mM H_2O_2	OD_{600} at 0.3 and 0.8
Mutant: Δ*fur*	a) 105 mM nitrate b) 250 mM salt c) 5 μM Fe d) 10 μM Fe e) 60 μM Fe	0, 30, 60, 120, 240 0, 30, 60, 120, 240 Exponential & stationary phase Exponential & stationary phase OD_{600} at 0.3 and 0.8,

Figure 2.4.1 Standard vs. Comparative microarray data. The blue line represents a standard microarray result for a gene that only measures change in expression. The microarray technique used in this study (quoted above) allows further differentiation through normalization of the RNA signal to genomic DNA allowing relative expression levels to be discerned, along with relative change. The yellow and purple lines represent high and low levels of basal expression, respectively, that would not otherwise be differentiated in a standard microarray. Note: The X-axis is not to scale.

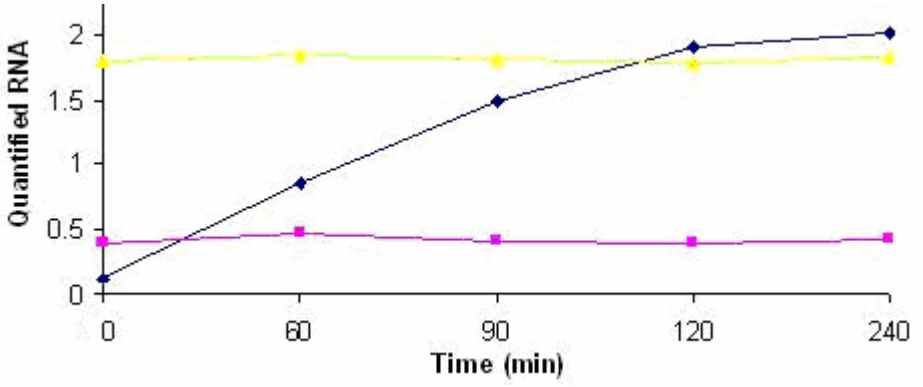
Quantified RNA
2
1.5
1
0.5
0
0
60
90
120
240
Time (min)

2.6 Growth Curves

All growth curves were conducted in rubber stoppered 16 x 125 mm screwcapped tubes. Ten ml of medium was inoculated with 0.2 ml of late logarithmic or early stationary phase cells grown overnight in Yen45 lactate / sulfate medium. The head space was less than 5 ml and was composed of 95% nitrogen and 5% hydrogen mix, the same gas mixture as the anaerobic chamber environment. All anaerobic manipulations were performed in a Coy anaerobic chamber (Coy Laboratory Products, Inc., Grass Lake, MI). Optical densities of the cultures in rubber stoppered tubes were taken at 600 nm on a GENESYS 20 Visible Spectrophotometer (Thermo Scientific, Waltham, MA).

2.7 DNA Isolation

Plasmid isolations were performed in accordance with the QIAprep Spin Miniprep Kit Protocol from the QIAgen Miniprep kit (Qiagen, Valencia, CA).

Genomic DNA isolations from *D. vulgaris* and *E. coli* were performed in accordance with the protocol provided with the Promega Wizard Genomic Preparation kit (Promega, Madison, WI) with the sole exception of the pellet being frozen before initiating the rest of the DNA isolation (Joe Ringbauer, unpublished).

2.8 Transformation

Transformation of *E. coli* α-select Bronze Efficiency cells (Bioline, Randolph, MA) or *E. coli* One Shot Top10 cells (Invitrogen, Carlsbad, CA) that were hosts for Topo vectors (Invitrogen, Carlsbad, CA) were accomplished in accordance with the instructions of the manufacturer. Aliquots of 10, 50, and 100 µl of recovered cells were plated onto solidified LC medium with the appropriate antibiotics for selection of transformants.

2.9 Electroporation

Electroporation of *D. vulgaris* was performed in accordance with the following protocol (Grant Zane, unpublished). One ml of culture freezer stock (early stationary phase cells in growth medium amended with 10% (v/v) glycerol) was placed in 9 ml of lactate / sulfite medium and grown anaerobically overnight at 34^{o}C. In the morning, 45 ml of lactate / sulfite medium was inoculated with 5 ml of the overnight culture and grown until an OD_{600} of ~0.30. The culture was centrifuged at 4 k rpm in an Accuspin 3R centrifuge with swinging bucket rotor (Fisher, Pittsburgh, PA) for 10 min and with the cells kept at either 4^{o}C or on ice at all times. The pelletted cells were resuspended in 35 ml of chilled (4^{o}C) electroporation buffer (EP) (30 ml 1M PIPES, 970 ml dH_20, pH adjusted to 7.2 with NaOH). The 4K rpm 10 min centrifugation was repeated and the cell pellet resuspended in 500 µl of EP buffer. 50 µl of resuspended cells were mixed with no more than 5 µl of the plasmid to be transformed and the mixture transferred to an electroporation cuvette (Molecular BioProducts cuvettes #5510, Fisher, Pittsburgh, PA). The sample in the cuvette was electroporated anaerobically with voltage and time constants of 1650 V and 250 ms, respectively. Samples that sparked, evidenced by a louder pop, visible flash, and the cap of the cuvette usually popping off, during electroporation had higher successful transformation rates (Grant Zane, unpublished). After electroporation, 1 ml of lactate / sulfite (amended with 1 g of yeast extract/liter) was added and the entire mixture transferred to a 1.5 ml microcentrifuge tube. The cells were allowed to recover anaerobically overnight at 34^{o}C and then plated with antibiotics for selection of transformants.

2.10 Strains, Plasmids, and Primers

Table 2.8.1 Strains created and modified.

[A] Name, how the strain will be referenced throughout this document.

[B] Parent Strain, the original strain that mutants were constructed from.

[C] Description, alterations performed on the Parent Strain to create the mutant.

[D] Source, origin of the mutant.

Name [A]	Parent Strain [B]	Description [C]	Source [D]
Desulfovibrio vulgaris Hildenborough ATCC29579	N/A	wild type w/ Native Plasmid (pDV1)	ATCC
JW801	*Desulfovibrio vulgaris* Hildenborough ATCC#29579 cured of pDV1	wild type	Wall lab
Desulfovibrio desulfuricans G20	*Desulfovibrio desulfuricans* G100A	Nal^R and cured of the cryptic plasmid pBG1	
JW0403	JW801	ΔDVU2792 (Δ*rnfC*)	This work
JW0405	JW801	ΔDVU1217 (Δ*norM1)*	This work
JW0407	JW801	ΔDVUA0164 (cation difusion facilitator)	This work
JW0409	JW801	ΔDVU2555 (Δ*norM2)*	This work
JW0411	JW801	ΔDVUA0095 (hypothetical gene)	This work
JW0413	JW801	ΔDVU0303/DVU0304 (hypothetical operon)	This work
JW0415	JW801	ΔDVU2791 (Δ*dhcA)*	This work
E. coli TG1	*E. coli* K12	Δ(*lac-pro*) *supE thi hsd*Δ *5*/F'*traD*36 *proA*$^+$*B*$^+$ *lacI*^{q} *lacZ*ΔM15	Yuji Morita (Morita et al., 1998)
E. coli Kam3	*E. coli* TG1	Δ(*lac-pro*) *supE thi (hsd)*Δ *5*/F'*traD*36 *proA*$^+$*B*$^+$ *lacI*^{q} *lacZ*ΔM15 Δ*acrAB*	Yuji Morita (Morita et al., 1998)
E. coli GG196	*E. coli* W3110	Δ*FieF*::cat	Gregor Grass (Grass *et al*., 2005)
E. coli GG200	*E. coli* W3110	Δ*FieF*::cat Δ*Fur*	Gregor Grass (Grass *et al*., 2005)
E. coli One Shot Top10	N/A	F- *mcr*A Δ(*mrr-hsd*RMS-*mcr*BC) φ80*lac*ZΔM15 Δ*lac*X74 *rec*A1 *ara*D139 Δ(*araleu*) 7697 *gal*U *gal*K *rps*L (StrR) *end*A1 *nup*G	Invitrogen
E.coli α-select Bronze Efficiency	N/A	deo^R *endA*1 *recA*1 *relA*1 *gyrA*96 *hsdR*17(rk -mk+) *supE*44 *thi*-1 Δ(*lacZYA-argFV*169) φ80*dlacZ*ΔM15 F-	Bioline

Table 2.8.2 Plasmids created and modified.

[A] Name, how the strain will be referenced throughout this document.

[B] Parent Plasmid, the original strain that mutants were constructed from.

[C] Description, alterations performed on the Parent Plasmid to create the mutant.

[D] Source, origin of the plasmid.

Name [A]	Parent Plasmid [B]	Source [C]	Description / Function [D]
pCR8-TOPO	N/A	Invitrogen	Topo isomerase plasmid by Invitrogen w/ Spectomycin resistance gene
Zero Blunt TOPO	N/A	Invitrogen	Topo isomerase plasmid by Invitrogen w/ kanamycin resistance gene
pBluescript	N/A	Fermentas	cut w/ EcoRV
pMO402	pBluescript	This work	suicide vector for creation of JW0403
pMO404	pBluescript	This work	suicide vector for creation of JW0405
pMO406	pBluescript	This work	suicide vector for creation of JW0407
pMO408	pBluescript	This work	suicide vector for creation of JW0409
pMO410	pCR8-TOPO	This work	suicide vector for creation of JW0411
pMO412	pCR8-TOPO	This work	suicide vector for creation of JW0413
pMO414	pCR8-TOPO	This work	suicide vector for creation of JW0415
pNorm1	Zero Blunt TOPO	This work	complementation of DVU1217 in *E. coli*
pNorm2	Zero Blunt TOPO	This work	complementation of DVU2555 in *E. coli*

Table 2.8.3 Primers created. Note that these are only the unique primer sequences for each marker exchange deletion. The full sequences are designated below with XXX replacing the sequence shown in the table and the JW04## designated to show which marker exchange mutant vector these were used to create. Figure 2.2.1 visually diagrams the sequences common to the primers as listed below:

JW04##-2: AAGACTGTAGCCGTACCTCGAATCTA (upstream common) XXX(gene upstream)

JW04##-3: AATCCGCTCACTAAGTTCATAGACCG(downstream common) XXX(gene downstream)

JW04##-5: TAGATTCGAGGTACGGCTACAGTCTT(upstream common) XXX(unique barcode) CCCCAGAGTCCCGCTCAG(kanamycin gene primer)

JW04##-6: CGGTCTATGAACTTAGTGAGCGGATT XXX(unique barcode) GAGGTAGCTTGCAGTGGGCT (kanamycin gene primer)

Name	Sequence (5' - 3')	Description
kan_N	CTCATCCTGTCTCTTGATCAGATCT	sequencing primer from N-term of kanamycin resistance gene
kan_C	CTACCCGTGATATTGCTGAAGAG	sequencing primer from C-term of kanamycin resistance gene
kan_int_F	AGATCTGATCAAGAGACAGGATGAG	generates an internal fragment of kanamycin resistance gene
kan_int_R	CTCTTCAGCAATATCACGGGTAG	generates an internal fragment of kanamycin resistance gene
TOPO8_F	AACGACGGCCAGTCTTAAGC	sequencing primer from multicloning site in pCR8-TOPO
TOPO8_R	AGACACGGGCCAGAGCTG	sequencing primer from multicloning site in pCR8-TOPO
JW0403-1	CGCAGACTATGCAGTACCCTGTGA	ΔDVU2792; Δ*rnfC*
JW0403-2	CATGGTGGTTCTTACCTTATTTCAGGTGGC	ΔDVU2792; Δ*rnfC*
JW0403-3	TAGGATGCGCCCGCCCGCA	ΔDVU2792; Δ*rnfC*
JW0403-4	AGCAGCGTGGAACCTGTCAG	ΔDVU2792; Δ*rnfC*
JW0403-5	CTGTCGGAATATAGGATACG	ΔDVU2792; Δ*rnfC*
JW0403-6	CAGACGAACTTAGATCACCG	ΔDVU2792; Δ*rnfC*
JW0405-1	GTGATGACCTGCATGCACGC	ΔDVU1217; Δ*norM1*
JW0405-2	CATGGATACCTTGTCACGGCCTCA	ΔDVU1217; Δ*norM1*
JW0405-3	TGACGATCCATCGAGGTCTGATTGT	ΔDVU1217; Δ*norM1*
JW0405-4	ACGCCGACGACAGAGCAC	ΔDVU1217; Δ*norM1*
JW0405-5	AGGATCTCAAAGTTGTCGAG	ΔDVU1217; Δ*norM1*
JW0405-6	ATCGCTCTAACCGTCGGAGA	ΔDVU1217; Δ*norM1*
JW0407-1	GGTCAGCAATCTCCCTACCAT	ΔDVUA0164; cation difusion facilitator
JW0407-2	CATCATCCGTCGCACATCCTTC	ΔDVUA0164; cation difusion facilitator
JW0407-3	TAGGGGCCCTGCGTACGGTTCAG	ΔDVUA0164; cation difusion facilitator
JW0407-4	ATTCTCGAAGAACCCATCCGCTT	ΔDVUA0164; cation difusion facilitator
JW0407-5	CGAATACGAGCAGATACGCG	ΔDVUA0164; cation difusion facilitator
JW0407-6	TCGTTTACCTGTCGCGCTGA	ΔDVUA0164; cation difusion facilitator
JW0409-1	GCACTGCGCGAGGGAGACAC	ΔDVU2555; Δ*norM2*
JW0409-2	CACGCCTGTGCCTTCCGCCGATG	ΔDVU2555; Δ*norM2*
JW0409-3	TGATTTCTCGCCCGTCACCCTCGA	ΔDVU2555; Δ*norM2*
JW0409-4	GACCGTGCTACACGGGAGCGAT	ΔDVU2555; Δ*norM2*
JW0409-5	AGGAACGTAACCATCAGTCC	ΔDVU2555; Δ*norM2*
JW0409-6	ACGGACAAATACGCACCTGT	ΔDVU2555; Δ*norM2*
JW0411-1	CAGGCGTCTGATGTCCGCATCGG	ΔDVUA0095; hypothetical gene
JW0411-2	ACGGCGAACCTTCAGGATTGCCTG	ΔDVUA0095; hypothetical gene
JW0411-3	TGCAACTGTGACAGGTTGAACCGC	ΔDVUA0095; hypothetical gene
JW0411-4	CCGGCCTCGAACGCCGAGAGA	ΔDVUA0095; hypothetical gene
JW0411-5	GTGCGGTAGACTCGTTCACT	ΔDVUA0095; hypothetical gene
JW0411-6	CACGTTTCAACTCGATTACG	ΔDVUA0095; hypothetical gene
JW0413-1	CGCTGGTAGGCGAACCCCTG	ΔDVU0303/DVU0304; hypothetical operon
JW0413-2	GACGGGCTCCTTGGTTTGTATGGAACC	ΔDVU0303/DVU0304; hypothetical operon
JW0413-3	CATCGCCACCGCAGTCCACC	ΔDVU0303/DVU0304; hypothetical operon

JW0413-4	GACGGCGTCCTTGGTGTCCT	ΔDVU0303/DVU0304; hypothetical operon
JW0413-5	CTGGCTTTACACGTACTGAG	ΔDVU0303/DVU0304; hypothetical operon
JW0413-6	AACTACAGAAACTTCGCTCG	ΔDVU0303/DVU0304; hypothetical operon
JW0415-1	CCATGCCTACATGGGCTGGTAC	ΔDVU2791; Δ*dhcA*
JW0415-2	TGCATGGACATTGGCATGTTGTGAG	ΔDVU2791; Δ*dhcA*
JW0415-3	ACCACCATGAGACAGCGTTTCCA	ΔDVU2791; Δ*dhcA*
JW0415-4	TGGCGATGGTGAGCACCGTCT	ΔDVU2791; Δ*dhcA*
JW0415-5	GTCTGCGTACCAGTCTGCAT	ΔDVU2791; Δ*dhcA*
JW0415-6	AGCGGTTTAACGTCAACGCA	ΔDVU2791; Δ*dhcA*

Chapter 3

EVALUATION OF STRESS RESPONSE IN SULFATE-REDUCING BACTERIA THROUGH GENOME ANALYSIS

3.1 Introduction

It is necessary to have a comprehensive understanding of the basic metabolism of the sulfate-reducing bacteria before these bacteria can be productively used as efficient agents for bioremediation of toxic compounds. In their environment, the SRB encounter a wide range of conditions to which they must adjust for survival. The availability of the genome sequence *D. vulgaris* Hildenborough has made possible transcriptional analysis of bacteria in a variety of growth conditions. An understanding of the basic levels of expression for "housekeeping" genes of these bacteria provides a foundation for comparison of differential gene expression obtained when stress conditions are imposed. Beyond the generalized expression profiles, details providing new understanding about nitrate, nitrite, and salt stresses were elucidated. Also, a new study was initiated discerning the roles of hypothetical genes in stress treatments in *D. vulgaris.* These research initiatives and the consequences of the results to the knowledge base of the SRB are discussed in detail throughout this and the following chapter.

3.2 Stress Experiment Conditions

In this study, wild type *D. vulgaris* Hildenborough cells were subjected to the 11 treatment conditions listed in Table 3.2.1, most of which were applied when the cells were in mid-exponential phase (OD_{600} = 0.3). To standardize the extent of the stress upon the cells, a treatment time or concentration that generated a 50% decrease in growth rate was chosen. An example of this growth rate is shown in Fig 3.2.1, demonstrated by

NaCl and KCl treatments. A sample was taken at initiation of the treatment and at time points up to six hours later. These conditions are summarized in Table 3.2.1 and treatment protocols are detailed in Chapter 2.4.

3.3 Computational Analysis

The microarray intensities obtained from cells treated with the 11 stresses were initially calculated as a $\log_2$R ratio (R is the ratio of experimental transcript to the control) and then Z scores were calculated using the formula and methodology detailed in Chapter 2.4 to determine statistical relevance. Genes with a Z score meeting the statistical level, abs(Z) $\geq$ 2, were considered for differential regulation and were the only ones used for further study. Fig. 3.3.1 lists the number of genes considered either increased or decreased, across the stress conditions. Approximately 65% of the 3482 *D. vulgaris* genes covered in the oligo microarrays exhibited differential regulation. Although the majority of the genome is regulated under some stress condition, the actual number of genes responding to a given stress varied depending on the particular stress condition.

Determining overlap between the stress responses allowed further insight into the interrelationship of stress responses by these bacteria. Direct comparisons were made between all the listed conditions in Fig. 3.2.1. To obtain the number of genes apparently regulated in multiple stresses, only genes regulated in the same direction were included in the final count (Table 3.3.1). Cold Shock, Salt, and Nitrate/Nitrite stresses are discussed in some detail below. The remaining treatments have been analyzed by collaborators and presented in other published articles; heat shock (Chhabra *et al*., 2006), pH (Stolyar *et al*.,

Figure 3.2.1 Wild type *D. vulgaris* in LS4 (black stars) and 250 mM NaCl (open red squares) and 250 mM KCl (open red triangles) (reproduced from Mukhopadhyay *et al.*, 2007).

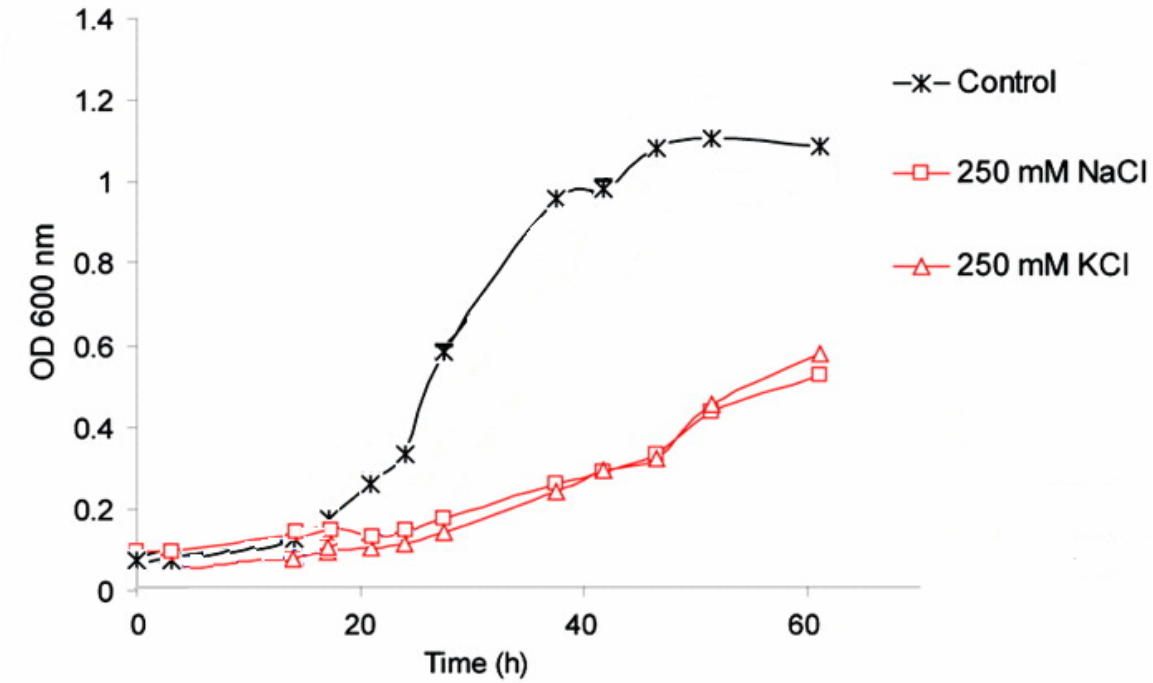
1.4
1.2
1
0.8
0.6
0.4
0.2
0
OD 600 nm
0
20
40
60
Time (h)
Control
250 mM NaCl
250 mM KCl

Table 3.2.1 Microarray conditions (reproduced from Barton and Hamilton, 2007).

[A] Stationary phase cells at 0.8 OD_{600} were compared to exponential phase cells at 0.3 OD_{600}. These OD_{600} levels are representative of these growth stages.

Stressor	Concentration or Condition	Time of sample (min)	Control culture
Cold	8ºC	240	30ºC, 240 min
Heat	50ºC	15	37ºC, 15 min
Oxygen	0.1 %	240	No O_2, 240 min
Alkaline pH	pH 10	120	pH 7, 0 min
Acid pH	pH 5.5	240	pH 7, 0 min
Nitrite	2.5 mM	60	No NO_2^-, 60 min
Nitrate	105 mM	240	No NO_3^-, 240 min
Sodium	250 mM	120	No added Na^+, 120 min
Potassium	250 mM	120	No added K^+, 120 min
Chromate	0.55 mM	120	No $CrO_4^=$, 0 time
Stationary[A]	0.8 OD_{600}		0.3 OD_{600}

Figure 3.3.1 Numbers of putative genes differentially expressed in response to stress conditions at the treatment times listed in Table 3.2.1 (red = increased, blue = decreased) (bars are additive, not overlapping) (reproduced from Barton and Hamilton, 2007).

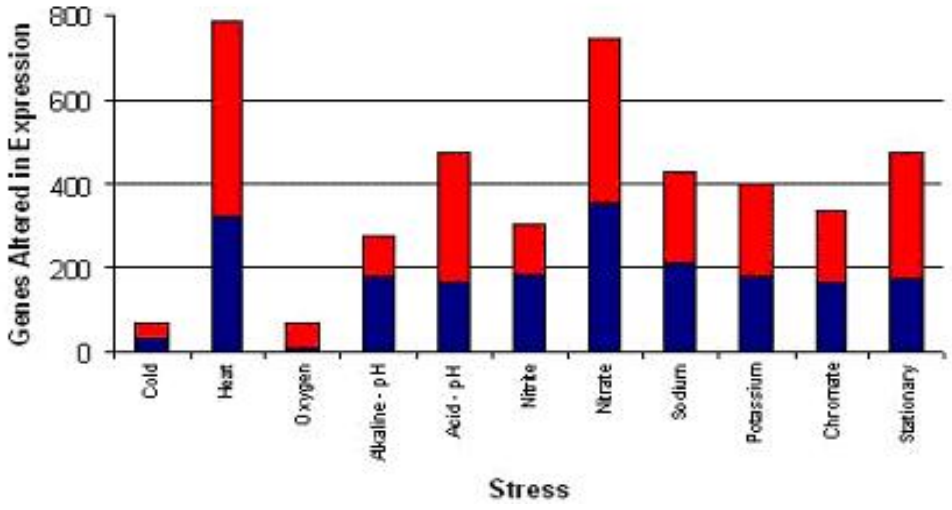
Genes Altered in Expression
800
600
400
200
0
Cold
Heat
Oxygen
Alkaline - pH
Acid - pH
Nitrite
Nitrate
Sodium
Potassium
Chromate
Stationary
Stress

Table 3.3.1 Numbers of genes similarly altered in regulation in two different treatments (treatments are described in Table 3.2.1) (recreated from Barton and Hamilton, 2007).

Treatments											
	Cold	Heat	O_2	pH10	pH5.5	NO_2^-	NO_3^-	NaCl	KCl	$CrO_4^=$	Stationary
Cold	68	*11*	*4*	*1*	*1*	*3*	*9*	*35*	*32*	*1*	*4*
Heat		785	*9*	*47*	*132*	*89*	*105*	*101*	*102*	*122*	*103*
O_2			70	*3*	*9*	*4*	*21*	*7*	*6*	*3*	*1*
pH10				280	*73*	*15*	*95*	*25*	*29*	*78*	*79*
pH5.5					471	*32*	*125*	*27*	*29*	*154*	*69*
NO_2^-						305	*36*	*19*	*15*	*22*	*39*
NO_3^-							742	*59*	*70*	*105*	*95*
NaCl								428	*254*	*33*	*24*
KCl									399	*37*	*28*
$CrO_4^=$										337	*57*
Stationary											470

2007), oxygen (Mukhopadhyay *et al*., 2007), chromium (Klonowska *et al.*, 2008) and stationary phase (Clark *et al.*, 2007).

3.4 Cold Shock

Low temperature shock was examined first because of the small subset of statistically significant differentially expressed genes. The *E. coli* cold shock response is known to be characterized by alterations in nucleic acid structure, ribosomes, and membrane fluidity (Phadtar, 2000). A sequence of events is initiated by protein YfiA and is followed by the production of a specialized set of cold shock proteins. Only a *yfiA* homolog was found in *D. vulgaris*, DVU1629, and unlike *E. coli* there was not a significant alteration in expression of this SRB gene during the cold treatment condition.

Other *D. vulgaris* genes found to be increased in expression were in similar categories to those found to be changed in cold-shocked *E. coli. D. vulgaris* has a single gene annotated as a 'cold shock protein' and showed negligible regulation to cold shock, but interestingly was up regulated, $\log_2 R = 1.4$, in heat shock. Genes associated with the ribosome and nucleic acid configuration also showed increased expression. For example, transcriptional increases were seen by genes encoding an RNA helicase (DVU3310), $\log_2 R = 1.8$; NusA (DVU0510) which, in *E. coli*, is a transcription terminator and part of an antitermination complex, $\log_2 R = 1.3$; translation initiation factor 2 (DVU0508), $\log_2 R = 1.1$; S17 (DVU1312), a ribosomal protein, $\log_2 R = 1.1$; and the UvrABC complex (DVU1987, DVU1605, DVU0801) used in the nucleotide excision repair pathway, $\log_2 R = 2.0, 2.1, 3.8$, respectively.

It was also observed that 15 / 68 of the differentially regulated genes were found to be annotated as having an involvement with the cell membrane. Strikingly, 35 of the

regulated genes were also similarly altered in expression in the high sodium stress condition; and slightly fewer, 32 genes, in the potassium treatment. Nine of those genes with expression profiles shared by the salt stresses are annotated as membrane related proteins, further showing the effect of all three stressors, cold, sodium and potassium, on the membrane.

3.5 Salt: Na^+ and K^+

Sodium and potassium stressed cells both had about 400 genes respond to increased salt concentrations. Between these two salt treatments approximately 65% of the differentially expressed genes were the same. Although the SRB had a larger number of differentially regulated genes in response to a lower concentration of potassium than sodium, 250 mM versus 500 mM respectively, the comparisons of these two cationic stresses to all other stressors shared a similar profile of common genes.

A number of genes involved in energy production showed expression increases as a consequence of salt exposure. These were: the ATP synthase operon (DVU0774-DVU0780) with respective $\log_2 R$ scores for sodium of 1.4, 1.2, 0.9, 1.0, 1.4, 1.7, 1.5; and potassium of 1.3, 1.7, 1.6, 1.5, 1.5, 1.5, 1.2; and the high molecular weight cytochrome operon (DVU0531-DVU0536) with respective $\log_2 R$ scores for sodium of 2.4, 1.3, 2.0, 1.1, 2.7, 3.0; and potassium of 2.0, 1.4, 2.3, 1.2, 1.5, 2.9. Increased energy might be required for active efflux of the sodium and potassium cations. Oddly, lactate permease genes, DVU2451 and DVU2683, sodium $\log_2 R = -1.7$ and $\log_2 R = -1.3$, potassium $\log_2 R = -2.3$ and $\log_2 R = -1.3$, respectively; and acetate kinase, DVU3030, sodium $\log_2 R = -2.3$ and potassium $\log_2 R = -2.3$, considered essential for energy production in lactate/sulfate

medium used for salt treatments, were down regulated creating a paradox in our understanding of the complete salt stress response.

3.6 Nitrate and Nitrite

Pockets of highly concentrated nitric acid are often found in contaminated areas where uranium or other heavy metal processing was performed, such as Hanford, WA. Thus, the effects of the addition of 105 mM nitrate (NO_3) or 2.5 mM nitrite (NO_2) on gene expression were determined to explore the putative mechanisms of *D. vulgaris* tolerance to these compounds. The pH was carefully controlled to eliminate gene changes primarily occurring to pHs outside of circumneutral ranges.

D. vulgaris lacks a nitrate reductase (Moura, 1997), and thus is incapable of using nitrate as a terminal electron acceptor or as a source of nitrogen. Identification of a specific sodium nitrate response was attempted by looking at a sum of the nitrite and sodium chloride response subsets. As seen in the Venn diagram (Fig. 3.6.1) the overlap is small in relation to the number of genes regulated in any single stress. The percentage of genes overlapping in any of the comparisons below was calculated as below what would have been expected at random: 1.0% (actual) versus 1.8% (random) for nitrate / nitrite overlap and 1.7% (actual) versus 2.5% (random) for nitrate / salt overlap. Actual percentages of genes changing in expression in common to two treatments were determined by dividing the number obtained from the microarray data by the total number of ORFs (3531 for *D. vulgaris*, microbesonline.org). The random percentages were calculated by multiplying the percentage of total genes differentially expressed in each individual treatment (21.0% of the total ORFs were changed in NO_3^-; 8.6% in NO_2^-; and 12.1% in salt). Because the overlap between these stresses is not higher that than

Figure 3.6.1 Venn diagram for $NaNO_3$ (Nitrate), $NaNO_2$ (Nitrite), and NaCl (Salt) overlap of regulated genes during stress response (reproduced from Barton and Hamilton, 2007).

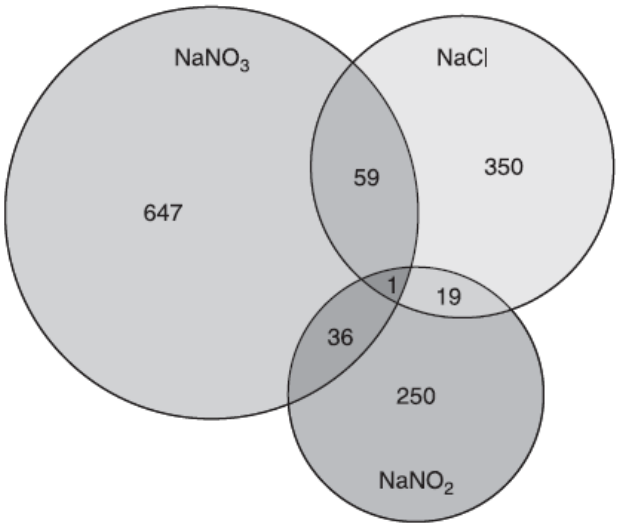
NaNO3
NaCl
647
59
350
1
19
36
250
NaNO2

Table 3.6.1 Nitrate expression unique groups (reproduced from Barton and Hamilton, 2007).

Transposases			Transporters		
Gene No.	Annotation	log_2R	Gene No.	Annotation	log_2R
DVU0556	ISDvu3, transposase OrfA	-2.23	DVU0088	Na+/pantothenate symporter	2.86
DVU0557	ISDvu3, transposase OrfB	-2.50	DVU0381	Na+/H+ aniporter NhaC-1	4.28
DVU0562	ISD1, transposase OrfA	-2.43	DVU0413	K^+ uptake, Trk1	1.43
DVU0564	ISDvu4, transposase truncation	-1.26	DVU0446	Na+/solute symporter family	1.52
DVU2010	ISD1, transposase OrfB	-1.64	DVU3108	Na+/H+ aniporter NhaC-2	5.13
DVU2017	ISDvu5, transposase	-1.95	DVU3332	Heavy metal P-type ATPase	2.23
DVU2004	ISDvu4, transposase	-1.72	DVU0177	*modA*, periplasmic protein, Mo ABC transporter	1.56
DVU2049	Transposase OrfA, IS3 family	-1.97	DVU0180	*modC,* ATP binding protein Mo ABC transporter	1.32
DVU2178	ISDvu2, transposase OrfB	-1.30			
DVU2179	ISDvu2, transposase, OrfA	-2.49			

expected by random between any given comparison, the response to nitrate is unique and not a sum of the nitrite and salt responses.

Several interesting groups of genes were noted to have coordinated, strong responses to nitrate. Ten transposase genes all showed statistically significant down regulation (Table 3.6.1). This group of genes was also regulated in the same fashion in response to acid and alkaline pH conditions. Ion transporter genes were up regulated, specifically those involved in Na^+ transport.

Although *D. vulgaris* lacks a nitrate reductase, it has a nitrite reductase, NrfA (DVU0625). Its function is believed to protect the cell from production of nitrite as intermediates from nitrate-reducing bacteria in the environmental community (Pereira, 2000; Greene, 2003). Deletion of the *nrfA* gene causes an increased sensitivity to nitrite (Haveman, 2004). The selection of genes that showed differential regulation in this study was in agreement with a small selection of genes studied in a nitrite response reported by Haveman and coworkers (2004). A down regulation of ATP synthase operons (DVU0774-80 and DVU0917-18), along with the DsrMKJOP operon (DVU1286-DVU1290). This Dsr complex is hypothesized to supply electrons to the sulfite reductase, DsrAB (DVU0402-DVU0403), which can be inhibited by nitrite (Wolfe, 1994). From these results, we hypothesize that redirection of electrons from a primary electron acceptor, sulfate or sulfite, to nitrite via nitrite reductase might interfere with the standard energetic respiration route that produces ATP or produce a reactive nitrogen species that inhibits the cell.

3.7 Conclusion

Our analysis has identified transcriptional relationships between the differing treatments and the gene regulation responses. Cold shock response included 15 genes associated with the cellular membrane being regulated. Curiously, close to half of the genes, 35, changed in expression to cold shock were also found to be regulated in response to salt treatment. Salt treatments shared an approximately two-thirds overlap between sodium and potassium treatments. Both stresses resulted in increased expression of energy generation operons that are postulated to be necessary to promote active efflux of the toxic concentrations of cations. Because nitrate cannot by used by *D. vulgaris* as a terminal electron acceptor or as a nitrogen source, it was tempting to expect that a nitrite response would be a simple composite of sodium and nitrite responses (Wall lab, unpublished results). However, the nitrate response exhibited a distinct regulation pattern of transposases and transporters, down- and up-regulated, respectively. The nitrite response was found to be similar to that reported in other published reports (Haveman, 2004), including down regulation of ATP synthase and an operon needed for sulfite reduction. Many of these relationships will necessitate further research to determine the exact nature of the response.

A major observation from the results of this microarray stress study was that there are a large number, 1237, of hypothetical genes that have significant roles in stress responses. The information obtained from these experiments would assist in assigning a function to some of the not yet annotated hypothetical genes still found in the genome of *D. vulgaris*.

The data discussed and figures shown in this chapter were published by Wall *et al*. in The Sulphate-reducing Bacteria, chapter 4: Evaluation of stress response in sulphate reducing bacteria through genome analysis, edited by Larry L. Barton and W. Allan Hamilton, 2007.

Chapter 4

CONFIRMATION AND CHARACTERIZATION OF HYPOTHETICAL GENES

4.1 Introduction

Over 35% of the predicted genes or open reading frames (ORFs) within the genome sequence of *Desulfovibrio vulgaris* Hildenborough (3,532 total) were not functionally annotated. These genes are described as encoding 'hypothetical proteins,' 'conserved hypothetical proteins,' or 'conserved domain proteins'. Such designations yield no information about the actual expression of the gene, the existence of the gene product, and no details about the protein function.

Microarray experiments measuring the transcriptional response of *D. vulgaris* at various growth states or stress conditions (currently 18 different treatments have been completed, see Table 2.4.1) have provided over 1,000,000 data points. Initial analysis of each experiment consistently shows differential expression of many of these unannotated genes. The primary objective of this analysis was to explore available data for evidence of expression of the predicted genes, those where RNA is actually transcribed, and, thus have an increased probability of producing functional proteins. These predictions must be further verified with current and future proteomics analyses of the same samples. After proving the existence of the proteins, predictions of their functions can profitably be made.

The secondary objective of this work was to construct a grouping of constitutively expressed hypothetical or conserved hypothetical proteins that might be candidates for function in basic metabolic pathways. Determining if these genes are essential or exert

an influence on metabolism will require construction of deletion mutants and phenotypic studies.

Third, genes encoding putative proteins were categorized by their conditional regulation in specific stress response conditions. Thus, transcriptional response to a given stress was inferred to indicate a potential functional role in that stress which might lead to a more specific metabolic assignment for these unannotated genes. Hints at function were also obtained by a comparison of the gene expression level to other genes in the same predicted operon and regulon. Thus "guilt by association" was inferred. Concomitantly, this study also examined operon predictions (Alm et al., 2005) through the correlated regulation profiles of the genes.

A more detailed understanding of the metabolic pathways of *D. vulgaris* is necessary to be able to fully harness its potential for environmental applications. Paving the way for future *in vivo* studies for over 1/3 of the genes is a critical aspect for the future research of the SRB as a viable bioremediation tool.

4.2 Analysis

'Hypothetical' proteins have been initially annotated as such because they lack sequence homology to any other known protein in any other life form and are purportedly unique to a particular organism. 'Conserved hypothetical' proteins have a homologue(s), usually found in related organisms. 'Conserved domain proteins' have a domain, a short contiguous stretch, within the protein sequence that is found in other organisms.

Seven functional categories determined by expression levels and responses to various treatments were created for initial clustering of these functionally unannotated genes (Table 4.2.1). These categories were then further subdivided for orphan genes,

those that are monocistronic, and those in operons. Finally separate considerations were made for 'hypothetical' versus 'conserved hypothetical / conserved domain' designations. Hypothetical genes in predicted operons that matched expression profiles of other genes in the operon were more readily annotated because of functional assignments of other operon members. Orphan hypothetical genes were more challenging to meaningfully annotate with anything more than a functional description because of the lack of more detailed physiological information, especially those in the 'expressed' or 'expressed, multiple stress response' categories.

Genes that fell into the 'no expression' category remained with their original 'hypothetical' or 'conserved hypothetical' designation. They cannot be discredited as bona fide genes for several reasons. The conditions requiring their expression may not have been studied, these genes may have faulty microarray spots preventing transcription monitoring or they might actually be genetic artifacts wrongly chosen by gene prediction software. Any of these reasons could cause this small subset of genes to remain annotated as 'hypothetical' or 'conserved hypothetical' until further dedicated studies that prove or disprove their existence.

4.3 Results

Tables containing all the hypothetical, conserved hypothetical and conserved domain genes in *D. vulgaris* are available in Appendix A. The DVU#, VIMSS#, response grouping, original annotation, and revised functional annotation are listed for each gene. The last two columns, 'Revised Functional Annotation; and 'Response Category,' are not used in the operon table for genes that already have a proper annotation.

Table 4.2.1 Functional grouping categories of unannotated genes of *D. vulgaris*

Category	**Definition**
no expression	No record of binding of the RNA to the oligonucleotide of the microarray in any control or stress experiments.
expressed	Differential expression was not detected and the basal expression level was not in the top 1/8 of expressed genes.
high expression	Differential expression was not detected and the basal expression level was in the top 1/8 of expressed genes.
expressed, single stress response	RNA level showed an absolute $\log_2$ (R) >= 1.2 change relative to the experimental control in a **single** stress condition and the basal expression level was **not** in the top 1/8 of expressed genes.
expressed, multiple stress response	RNA level showed an absolute $\log_2$ (R) >= 1.2 change relative to the experimental control in **multiple** stress conditions and the basal expression level was **not** in the top 1/8 of expressed genes.
high expression, single stress response	RNA level showed an absolute $\log_2$ (R) >= 1.2 change relative to the experimental control in a **single** stress conditions and the basal expression level was in the top 1/8 of expressed genes.
high expression, multiple stress response	RNA level showed an absolute $\log_2$ (R) >= 1.2 change relative to the experimental control in **multiple** stress conditions and the basal expression level was in the top 1/8 of expressed genes.

Figure 4.3.1 Break down of response categories of monocistronic hypothetical genes. Sample size of 680. Definitions of the categories are listed in Table 4.2.1 (reproduced from Elias *et al*., 2008).

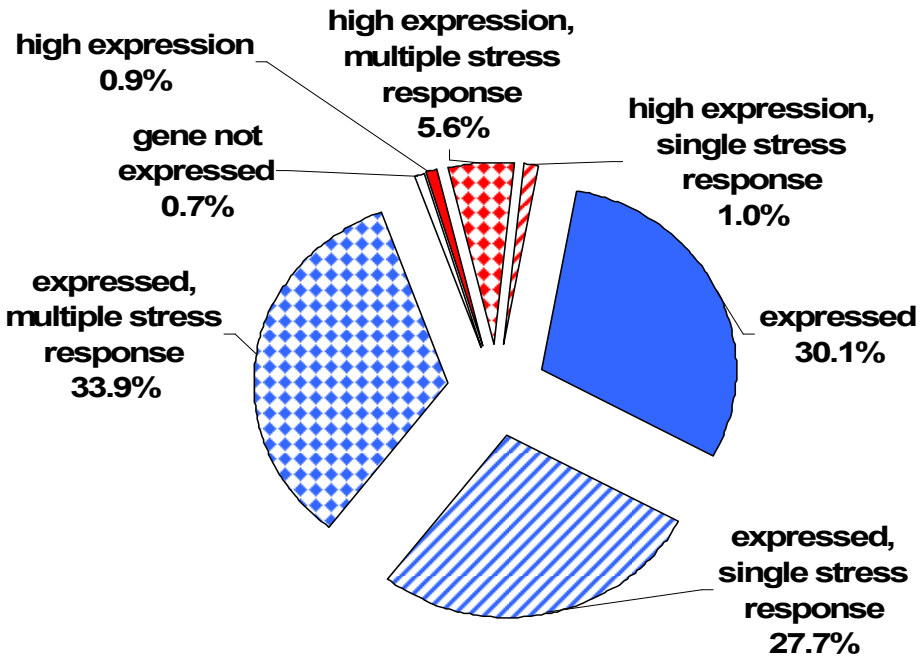
high expression
0.9%
high expression,
multiple stress
response
5.6%
high expression,
single stress
response
1.0%
gene not
expressed
0.7%
expressed,
multiple stress
response
33.9%
expressed
30.1%
expressed,
single stress
response
27.7%

Figure 4.3.2 Break down of response categories of hypothetical genes predicted to be in operons. Sample size of 557. Definitions of the categories are listed in Table 4.2.1 (reproduced from Elias *et al*., 2008).

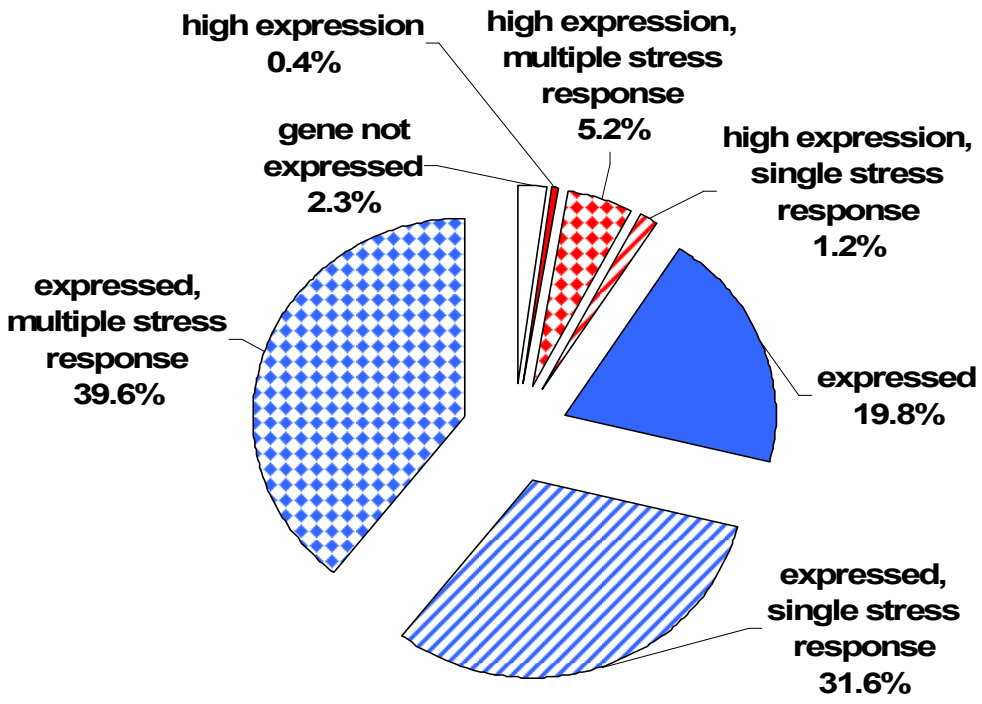
high expression
0.4%
high expression,
multiple stress
response
5.2%
gene not
expressed
2.3%
high expression,
single stress
response
1.2%
expressed,
multiple stress
response
39.6%
expressed
19.8%
expressed,
single stress
response
31.6%

These figures show the interconnected regulation of many genes in the genome by the large percentage of hypothetical genes that fall into the 'multiple stress response' category, 33.4%. This is in agreement with many of the operons containing hypothetical genes with 39.6% responding to multiple treatments.

To explore possible functional roles of these differentially expressed unannotated genes, two were selected from different categories: 'expressed, single stress response' and 'expressed, multiple stress response,' each from the monocistronic and operonic grouping, respectively. Deletion mutants of the selected genes, DVUA0095 and DVU0303/0304, were made and their phenotypes tested to verify whether the predictions made in this study contributed to an understanding of function for these genes as extrapolated from transcriptional responses. More deletions are being constructed and studied. Random transposon mutations in the genes identified as differentially expressed are also being examined for phenotypic characteristics.

The data and results discussed in this chapter have been submitted as a paper to Nucleic Acids Research in October 2008. The title is 'Expression profiling of hypothetical genes in *Desulfovibrio vulgaris* leads to improved functional annotation' and it was authored by Dwayne Elias *et al*. A full reference is included in the references section at the end of this document.

4.4 Physiology of Mutants

4.4.1 JW0411: Chromium Response Gene on pDV1

The deletion of VIMSS209626 (DVUA0095) was the first deletion constructed that was located on pDV1, the 202 kb native plasmid present in wild-type *D. vulgaris* Hildenborough. This ΔDVUA0095 strain was designated JW0411, and the deletion

removed the entire protein coding sequence. DVUA0095 is monocistronic and its transcription was differentially increased only in response to the addition of chromate. Interestingly, it is located adjacent to and divergently transcribed from a locus of two genes annotated as involved in chromate handling, *chrB*, encoding a conserved protein, and *chrA*, an apparent chromate transporter.

This hypothetical gene is the only gene of these three that shows significant regulation in chromium stress response, according to the microarray data (Fig.4.4.1.2). Further, this is the only stress condition to which any of these genes respond, although few data points were actually available for *chrA* or *chrB*.

The strong increase in transcription of DVUA0095 when challenged with chromate suggested that this gene might encode a protein functioning to protect cells against the toxic metal. Initial physiological analysis demonstrated the expected phenotype of increased chromium sensitivity in the JW0411 mutant compared to wild type. There was no discernable growth difference when the mutant was cultured in LS4 medium without chromate added.

After the addition of 0.40 mM and 0.45 mM potassium chromate (K_2CrSO_4), the JW0411 strain was able to grow after a lag period that increased in accordance to the concentration of stressor, approximately 50 and 100 hours, respectively, longer lag in comparison to wild type. These physiological results show a distinct chromium response phenotype of the mutant and the gene can thus be annotated more informatively.

Figure 4.4.1.1 Operon prediction for DVUA0095. Blue filled arrow represents DVUA0095 and the head of the arrow represents the direction of transcription. Numbers are the exact number of nucleotides between predicted genes. White arrows represent genes not part of an operon with DVUA0095.


chrB
DVLA0095
COG-AraJ
404
84

Figure 4.4.1.2 Heat map of the differential expression of DVUA0095 in response to chromate.. The numbers to the left represent the final concentration of sodium chromate in the treated cultures and the time of exposure. The colored boxes are coded for the level of differential transcription when compared with an untreated culture at the same growth stage. The column of boxes to the right is the color key for ratios of transcription of treated cells versus control. Dark outlines around the boxes indicate an absolute Z score of >2.0 for the data and white boxes are less than 2.0.

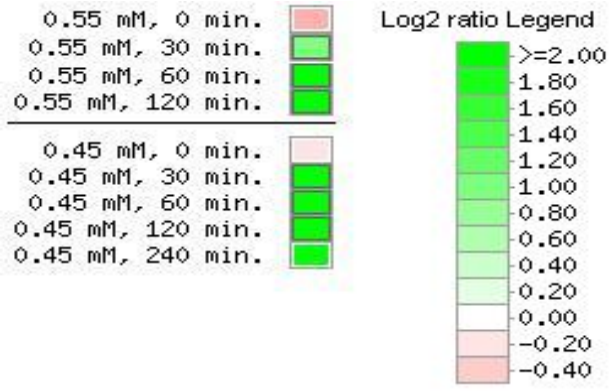
0.55 mM, 0 min.
0.55 mM, 30 min.
0.55 mM, 60 min.
0.55 mM, 120 min.
0.45 mM, 0 min.
0.45 mM, 30 min.
0.45 mM, 60 min.
0.45 mM, 120 min.
0.45 mM, 240 min.
Log2 ratio Legend
>=2.00
1.80
1.60
1.40
1.20
1.00
0.80
0.60
0.40
0.20
0.00
-0.20
-0.40

Figure 4.4.1.3 Growth curve of WT (red diamonds) and JW0411 (green triangles) in lactate / sulfate medium.

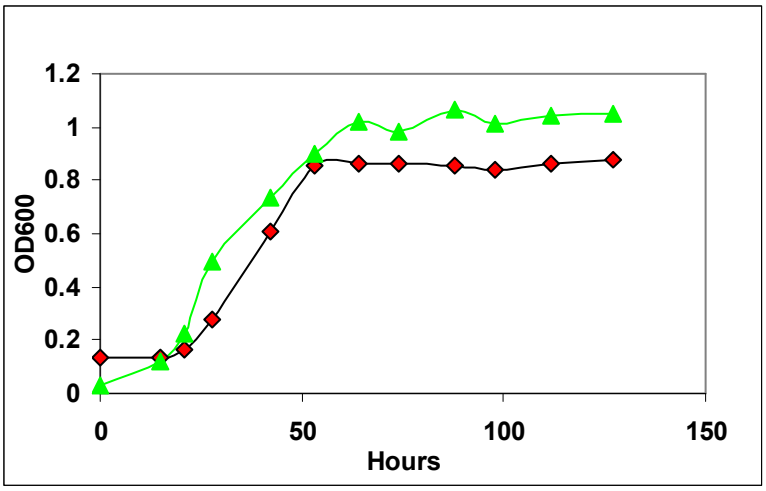
1.2
1
0.8
0.6
0.4
0.2
0
OD600
0
50
100
150
Hours

Figure 4.4.1.4 Growth curve of WT (red diamonds) and JW0411 (green triangles) with 0.40 mM potassium chromate (K_2CrO_4) added to lactate / sulfate grown cultures at zero time.

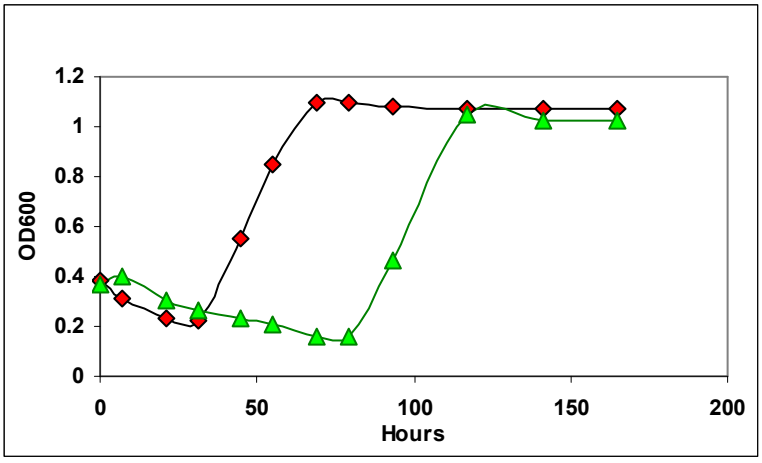
1.2
1
0.8
0.6
0.4
0.2
0
OD600
0
50
100
150
200
Hours

Figure 4.4.1.5 Growth curve of WT (red diamonds) and JW0411 (green triangles) with 0.45 mM potassium chromate (K_2CrO_4) added to lactate / sulfate grown cultures at zero time.

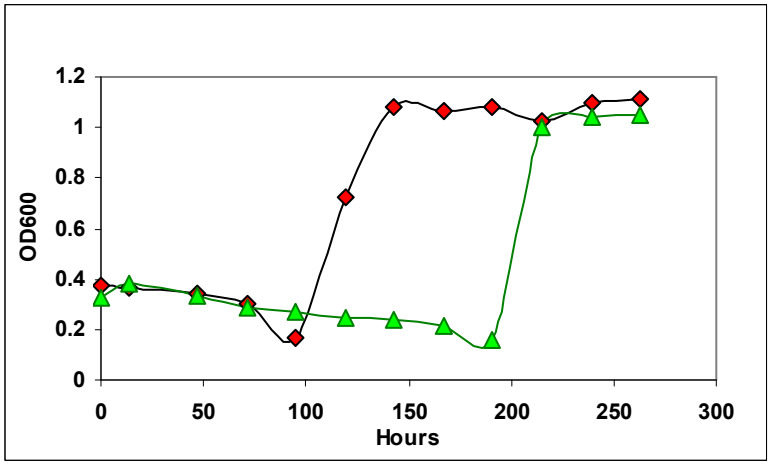
1.2
1
0.8
0.6
0.4
0.2
0
OD600
0
50
100
150
200
250
300
Hours

The mutant JW0411 is not impaired in growth on lactate / sulfate medium as illustrated in the growth curve shown in Fig. 4.4.1.3. The increased sensitivity of JW0411 to added chromate was interpreted to mean that the hypothetical protein encoded by DVUA0095 has some role in protecting *D. vulgaris* from the inhibitory effects of this toxic metal.

4.4.2 JW0413: Stress Response Couplet

The construction of a deletion mutant for VIMSS209237/209238 (DVU0303/0304) was the first two-gene deletion constructed in *D. vulgaris*. This ΔDVU0303/0304 strain is referred to as JW0413. The deletion is inclusive of the start codon of DVU0304 through the stop codon for DVU0303. DVU0303/0304 is a two gene operon with significant regulation across many stresses. This operon is one of two transcripts that have significant up regulation in at least six stresses; the other being *feoA*, a putative ferrous iron transport protein, DVU2572. It is interesting to note that the only conditions in which DVU0303/0304 is down regulated are in a culture lacking pDV1 or in coculture with *Methanosarcina*. Transcription of this couplet is increased in response to all growth inhibitory agents.

The mutant JW0413 is not impaired in growth on lactate/sulfate medium as illustrated by the growth curve shown in Fig. 4.4.2.4. Chromate at 0.45 mM caused an extended lag time beyond that of the WT by about 60 h even though the starting culture densities were quite similar. The most dramatic delay in growth occurred following the addition of 2 mM nitrite to the cultures. JW0413 was unable to grow significantly for over 16 days in this condition, while the WT grew to full cell density in about 10 days. Clearly the absence of the genes in this two gene operon causes the cells to be more

Figure 4.4.2.1 Operon prediction for DVU0303/DVU0304. Blue filled arrows represents DVU0303 and DVU0304 and the head of the arrow represents the direction of transcription. Numbers are the exact number of nucleotides between predicted genes. White arrows represent genes not part of the operon containing DVU0303/0304.


COG1406
DVU0303
DVU0304
fd II
348
31
130

Figure 4.4.2.2 Heat map for selected stress responses. The numbers to the left represent the final concentration of selected chemicals in the treated cultures and the time of exposure; DVU0303 differential expression is illustrated on the left and DVU0304 is on the right. The colored boxes are coded for the level of differential transcription when compared with an untreated culture at the same growth stage. The column of boxes under the heading "Log2 ratio Legend" is the color key for ratios of transcription of treated cells versus control. Dark outlines around the boxes indicate an absolute Z score of >2.0 for the data and white boxes are less than 2.0. pDV1 was referred to as the 'Megaplasmid' in the microarray studies.

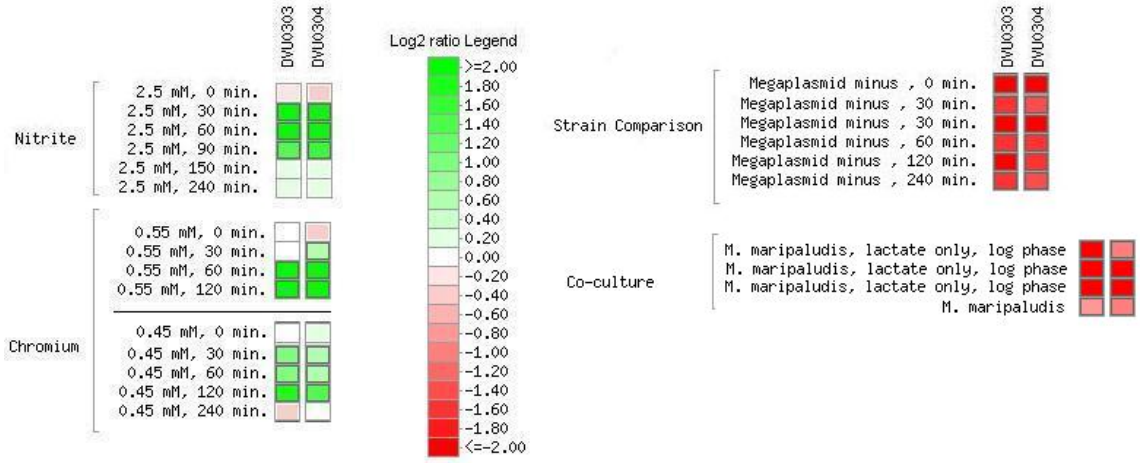
DWU0303
DWU0304
Nitrite
2.5 mM, 0 min.
2.5 mM, 30 min.
2.5 mM, 60 min.
2.5 mM, 90 min.
2.5 mM, 150 min.
2.5 mM, 240 min.
Chromium
0.55 mM, 0 min.
0.55 mM, 30 min.
0.55 mM, 60 min.
0.55 mM, 120 min.
0.45 mM, 0 min.
0.45 mM, 30 min.
0.45 mM, 60 min.
0.45 mM, 120 min.
0.45 mM, 240 min.
Log2 ratio Legend
>=2.00
1.80
1.60
1.40
1.20
1.00
0.80
0.60
0.40
0.20
0.00
-0.20
-0.40
-0.60
-0.80
-1.00
-1.20
-1.40
-1.60
-1.80
<=-2.00
Strain Comparison
Megaplasmid minus , 0 min.
Megaplasmid minus , 30 min.
Megaplasmid minus , 30 min.
Megaplasmid minus , 60 min.
Megaplasmid minus , 120 min.
Megaplasmid minus , 240 min.
Co-culture
M. maripaludis, lactate only, log phase
M. maripaludis, lactate only, log phase
M. maripaludis, lactate only, log phase
M. maripaludis

Figure 4.4.2.3 Growth curve of WT (red diamonds) and JW0413 (blue circles) in lactate / sulfate medium.

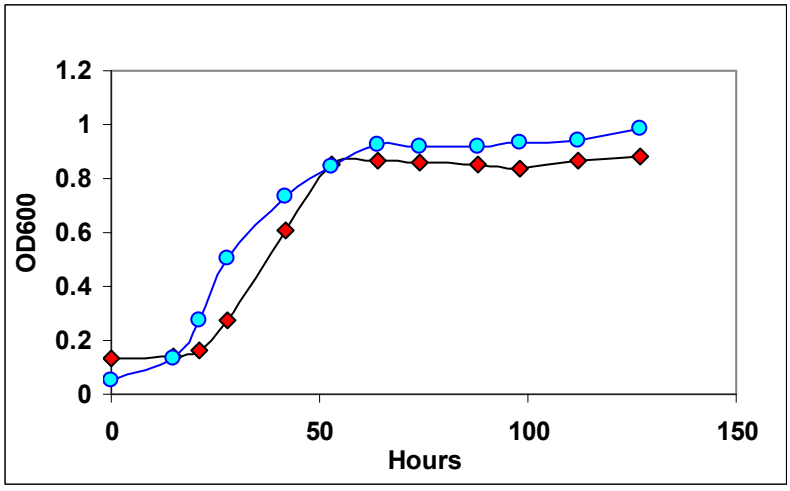
1.2
1
0.8
0.6
0.4
0.2
0
OD600
0
50
100
150
Hours

Figure 4.4.2.4 Growth curve of WT (red diamonds) and JW0413 (blue circles) with 0.45 mM potassium chromate (K_2CrO_4) added to cultures in lactate / sulfate medium at zero time.

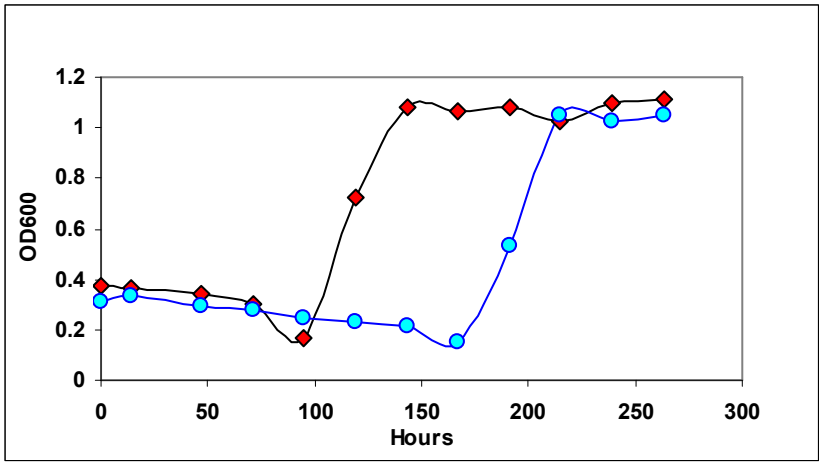
1.2
1
0.8
0.6
0.4
0.2
0
OD600
0
50
100
150
200
250
300
Hours

Figure 4.4.2.5 Growth curve of WT (red diamonds) and JW0413 (blue circles) with 2 mM nitrite ($NaNO_2$) added to cultures in lactate / sulfate medium at zero time.

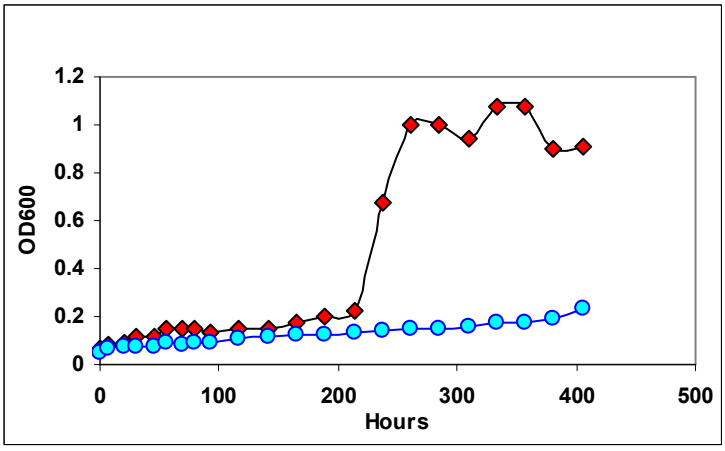
1.2
1
0.8
0.6
0.4
0.2
0
OD600
0
100
200
300
400
500
Hours

sensitive to these two inhibitory chemicals. The mechanism of this sensitivity will need further examination. It will also be of interest to determine whether this mutant is also more sensitive to exposure to oxygen or heat.

Chapter 5

ION TRANSPORT

5.1 Introduction

Ion transportation plays an integral role in cell biology. The functionality ranges from transport systems, efflux, and chemical signaling. Efflux and transfer systems are categorized in different groups depending on the energetic requirements for ion transfer (Silver, 1996) and whether other molecules are transported across membrane barriers along with the ion forming a motive force. Chemical signaling uses ion transport as an indicator to control metabolic pathways in response to suboptimal survival conditions (Tsuchiya *et al*., 1998). The ion transporters discussed in this chapter are involved in a diverse selection of the groupings briefly described above, but will focus on transport and efflux systems.

Three ion transport systems of *D. vulgaris* were identified as orthologs of systems from better studied bacteria. First, the NQR complex has been shown to be required for active nutrient uptake in marine bacteria through efflux of sodium ions (Hayashi *et al.*, 2000). Second, the NorM genes of *Vibrio parahaemolyticus* were shown to encode putative Na^+-dependent multidrug antiporters (Morita et al., 1998) that actively export various toxic compounds while taking in sodium ions. Third, DVU1778 (encoding a putative FieF protein for iron removal) and DVU0164 fall into the category of CDFs

(Nies and Silver, 1995), cation diffusion facilitators. This third, novel category encompasses metal ion transporters that may play a role in the resistance of *D. vulgaris* to toxic metals, such as chromium and be a key feature needed for success in bioremediation efforts. These novel ion efflux systems specific for metal ion resistance undergo significant regulation during stress treatments in *D. vulgaris*. These genes are discussed in depth and with specific regard to the physiology of *D. vulgaris* in the following sections.

5.2 RNF Operon

The *rnf* operon, identified from *Rhodobacter capsulatus*, was shown to be essential for nitrogen fixation (Jouanneau et al. 1998; Saeki and Kumagai, 1998). The operon purportedly produces a transmembrane transport system providing a conduit for electrons to access the nitrogenase enzyme. The *rnf* operon typically consists of 7 genes with conserved synteny in many microorganisms (Alm *et al*., 2005). *Vibrio cholerae* encodes a homologous seven gene operon designated *nqr* for Na^+-dependent NADH-quinone oxidoreductase complex (Jouanneau et al. 1998). This complex has been suggested to use primary metabolic energy to establish a sodium motive force that can be used to generate ATP or support motility (Unemoto *et al*., 2001).

A homologous operon was observed in the genome of *D. vulgaris*. The annotation in this sulfate reducer used the *rnf* naming system for the genes (TIGR), but also incorporated descriptions of the *nqr* complex components (Alm *et al*., 2005), leading to some confusion regarding its true function. *D. vulgaris* and *D. desulfuricans* G20 have a unique decaheme cytochrome, DhcA, and the gene encoding this cytochrome is predicted to be the first gene in the *rnf* operon (Alm et al., 2005). A *dhcA* gene is not

associated with the *rnf* or *nqr* operon in any other organism that has been sequenced or any published studies of any orthologous operons (Elliott Drury, unpublished).

Targeted deletions were constructed by marker exchange mutagenesis in *D. vulgaris* for *dhcA* and *rnfC*, the first and second genes in the operon, designated as strains JW0415 and JW0403, respectively.

The data from microarrays of *D. vulgaris* subjected to inhibitory stresses (Fig. 5.1.2) would generally support the inclusion of *dhcA* in the *rnf* operon. The coefficient of correlation for expression is a metric that scores the relationship of how closely the expression levels for the genes in this operon are related. The scores for the *rnf* operon ranged from 0.66 to 0.92 (Alm *et al*., 2005). Exposure to peroxide and salt showed no greater variability between *dhcA* and *rnfC* expression than was shown between other members of the predicted operon. It would be inferred that seven of the eight genes (*apbE*, the last gene in the putative operon and the exception of the eight) might function together to form an electron conduit across the membrane. If that were the case, then marker replacement mutations of either of the first two genes in the putative operon should result in the same phenotype, since this mutation should be polar. This was not found.

Construction of marker replacement deletion mutants were carried out for *rnfC,* DVU2792, and *dhcA*, DVU2791. They were completed in accordance with the materials and methods section. Primers and suicide vectors used are listed in Tables 2.8.2 and 2.8.3, respectively. The mutant strains of Δ*rnfC* and Δ*dhcA* were designated JW0403 and

Figure 5.1.1 Operon prediction for the *rnf* operon in *D. vulgaris*. The head of the arrow represents the direction of transcription, with the dark blue box representing DVU2792, *rnfC*; and the box immediately left of *rnfC* representing *dhcA*. The latter is predicted to be promoter proximal. The other light blue boxes to the right of *rnfC* are predicted to encode the rest of the operon. The white arrows represent genes not part of the operon and on the opposite strand.


dhcA
DVU2792
COG-RnfD
COG-Rn
nqr4
b1627
COG3075
COG-ApbE
51
14
138
3
12
10
70
-3
95

Figure 5.1.2 Heat maps of stress responses for the predicted *rnf* operon in *D. vulgaris*. The numbers to the left represent the final concentration of described stressor in the treated cultures and the time of exposure. The colored boxes are coded for the level of differential transcription when compared with an untreated culture at the same growth stage. The column of boxes in the middle is the color key for ratios of transcription of treated cells versus control.

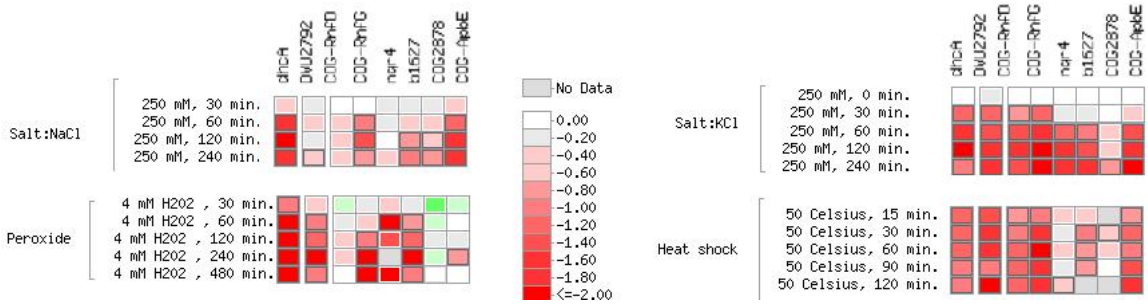
dnaA
DW2792
COG-RnfD
COG-RnfG
nar4
n1527
COG2878
COG-ApbE
Salt:NaCl
250 mM, 30 min.
250 mM, 60 min.
250 mM, 120 min.
250 mM, 240 min.
Peroxide
4 mM H202 , 30 min.
4 mM H202 , 60 min.
4 mM H202 , 120 min.
4 mM H202 , 240 min.
4 mM H202 , 480 min.
No Data
0.00
-0.20
-0.40
-0.60
-0.80
-1.00
-1.20
-1.40
-1.60
-1.80
<=-2.00
Salt:KCl
250 mM, 0 min.
250 mM, 30 min.
250 mM, 60 min.
250 mM, 120 min.
250 mM, 240 min.
Heat shock
50 Celsius, 15 min.
50 Celsius, 30 min.
50 Celsius, 60 min.
50 Celsius, 90 min.
50 Celsius, 120 min.

JW0415, respectively. The pMO402 deletion vector, for the Δ*dhcA* construct was found to have two nucleotide differences from the published *D. vulgaris* sequence. The first was a 'C' to 'T' mutation in the intergenic region downstream of the kanamycin marker. The second caused a serine to threonine change in the protein translated from the gene following *rnfC* in the operon. Neither of these were expected to alter the phenotype because the construction of the deletion by marker exchange was assumed to create a polar mutation interfering with the transcription of downstream genes. The pMO414 mutagenic vector for the Δ*dhcA* construct had a 'G' to 'A' transition mutation in the upstream "common sequence" introduced into all deletion constructs from the Wall laboratory. This nucleotide change was assumed to have a negligible effect on the physiology, but should be kept in mind should the "common sequences" be used for quantitative comparison of deletion fitness by PCR.

The growth of these two deletion strains, Δ*rnfC* and Δ*dhcA*, on dinitrogen as sole nitrogen source was tested. Fig. 5.1.3 shows the results for Δ*rnfC*, JW0403. This strain was impaired for nitrogen fixation, although JW0415, Δ*dhcA*, was not (data not shown). The nitrogen fixation of JW0403 was tested in a pyruvate / sulfite medium with N_2 as the sole nitrogen source. This medium was used rather than the standard lactate / sulfate medium because the latter requires the expenditure of two ATP equivalents for the activation of each sulfate before its reduction is possible (Postgate, 1984). Nitrogen fixation requires 16 moles of ATP per mole of N_2 reduced. When that energy demand is coupled with the necessity of activation of sulfate to provide a terminal electron acceptor, the cells sometimes cannot be observed to grow. The slower growth of the Δ*rnfC* mutant can easily be seen when compared to wild type nitrogen-fixing cultures, Fig. 5.1.3.

Figure 5.1.3 Pyruvate / sulfite growth with N_2; JW0403 (Δ*rnfC)* (green) and WT (red). The severely impaired growth of JW0403 compared to WT with N_2 as the sole nitrogen source confirms that the *rnfC* is necessary for nitrogen fixation.

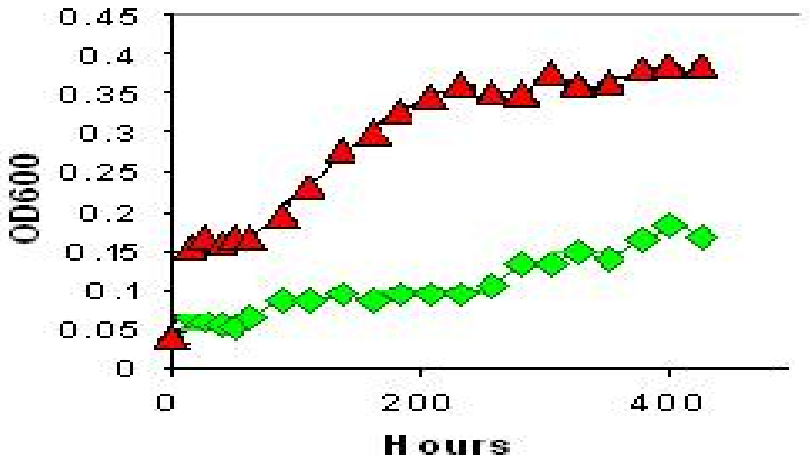
0.45
0.4
0.35
0.3
0.25
0.2
0.15
0.1
0.05
0
OD600
0
200
400
Hours

Other phenotypic growth results for JW0403 show a two day lag phase compared to wild type *D. vulgaris* when grown on lactate / sulfate (data not shown). JW0403 suffered impaired growth with ethanol as an electron donor when using sulfate or sulfite as a terminal electron acceptor, but not thiosulfate (data not shown). The latter may result from the overall slower rate of growth of all strains on ethanol / thiosulfate medium.

Surprisingly none of these physiological phenotypes were witnessed in the JW0415 strain. These data question the prediction that *dhcA* is part of the *rnf* operon. RT-PCR experiments are needed to explore the existence of a contiguous transcript containing sequences from both genes.

5.3 Cation Diffusion Facilitators (CDF)

The presence of several iron related response genes, *fur* (DVU0942) and *feoA* (DVU2572), being among the highest responding genes across a diverse range of stresses; along with DVU1778, a cation diffusion facilitator (CDF) gene, (Elliott Drury, unpublished) sparked an interest in iron studies. This latter *D. vulgaris* gene was a putative homolog a novel iron cation efflux gene, *fieF*, studied in *E. coli* (Grass et al., 2005). Published research on the *E. coli* gene provided some explanation for the absence of an expected excess iron in a mutant of *E. coli* lacking the Fur repressor in which the iron uptake systems are derepressed (Grass et al., 2005).

It was found that the *D. vulgaris* gene (DVU1778) has 51% homology over the protein sequence and an E-value of e^-28 (a ClustalW alignment is shown in Fig. 5.2.1) compared to the *E. coli fieF* gene. Curiously, the *D. vulgaris* homolog has an extra 160 amino acid carboxy terminal tail.

Figure 5.2.1 Clustal W alignment of *E. coli fieF* and *D. vulgaris* DVU1778. The results of the alignment show a 51% similarity across the entire protein.

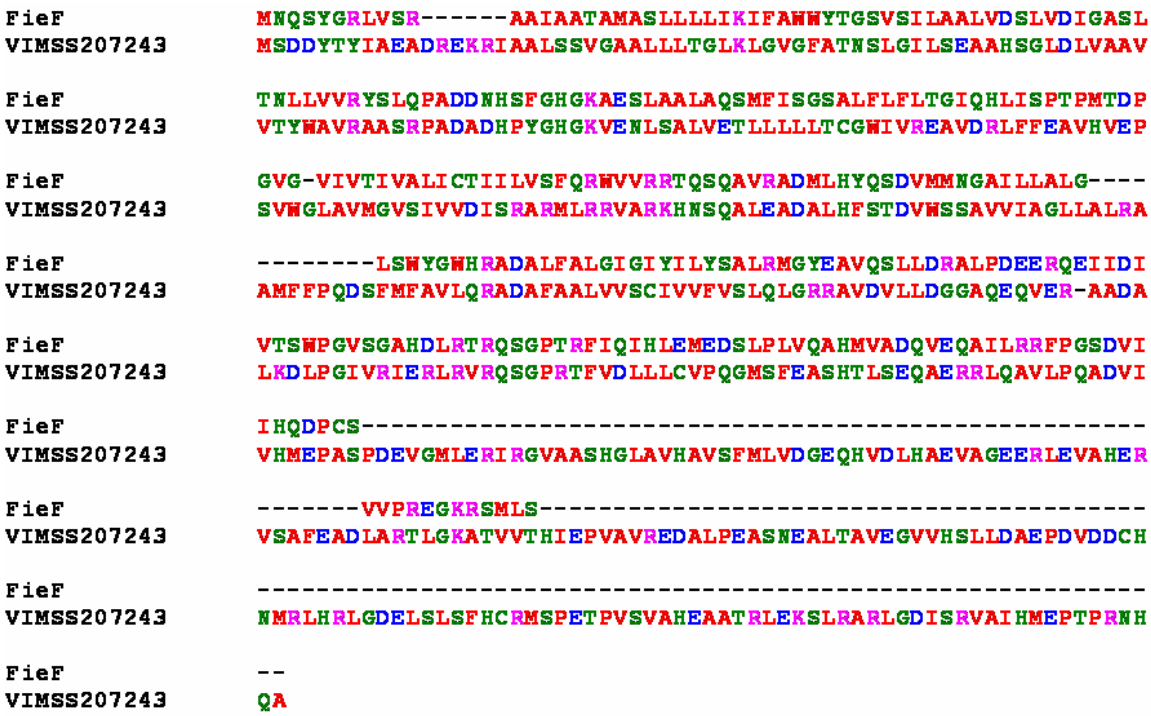
FieF MNQSYGRLVSR------AAIAATAMASLLLLIKIFAWWYTGSVSILAALVDSLVDIGASL
VIMSS207243 MSDDYTYIAEADREKRIAALSSVGAALLLTGLKLGVGFATNSLGILSEAAHSGLDLVAAV
FieF TNLLVVRYSLQPADDNHSFGHGKAESLAALAQSMFISGSALFLFLTGIQHLISPTPMTDP
VIMSS207243 VTYWAVRAASRPADADHPYGHGKVENLSALVETLLLLLTCGWIVREAVDRLFFEAVHVEP
FieF GVG-VIVTIVALICTIILVSFQRWVVRRTQSQAVRADMLHYQSDVMMNGAILLALG----
VIMSS207243 SVWGLAVMGVSIVVDISRARMLRRVARKHNSQALEADALHFSTDVWSSAVVIAGLLALRA
FieF --------LSWYGWHRADALFALGIGIYILYSALRMGYEAVQSLLDRALPDEERQEIIDI
VIMSS207243 AMFFPQDSFMFAVLQRADAFAALVVSCIVVFVSLQLGRRAVDVLLDGGAQEQVER-AADA
FieF VTSWPGVSGAHDLRTRQSGPTRFIQIHLEMEDSLPLVQAHMVADQVEQAILRRFPGSDVI
VIMSS207243 LKDLPGIVRIERLRVRQSGPRTFVDLLLCVPQGMSFEASHTLSEQAERRLQAVLPQADVI
FieF IHQDPCS----------
VIMSS207243 VHMEPASPDEVGMLERIRGVAASHGLAVHAVSFMLVDGEQHVDLHAEVAGEERLEVAHER
FieF -------VVPREGKRSMLS----------
VIMSS207243 VSAFEADLARTLGKATVVTHIEPVAVREDALPEASNEALTAVEGVVHSLLDAEPDVDDCH
FieF ----------
VIMSS207243 NMRLHRLGDELSLSFHCRMSPETPVSVAHEAATRLEKSLRARLGDISRVAIHMEPTPRNH
FieF --
VIMSS207243 QA

In microarray analyses of differential gene expression in *D. vulgaris* subjected to various growth-limiting treatments, the *fieF* ortholog, DVU1778, was seen significantly (Z score >= absolute(2)) down regulated; for example, with high salt or nitrate, at acidic pH, or exposed to peroxide or chromium (Fig 5.2.2; Alm et al., 2005). This gene was also decreased in expression during stationary versus exponential phase of growth.

Grass et al. (2005) showed that the phenotype of a deletion of *fieF* was consistent with a role for this gene in relieving intracellular iron toxicity in *E. coli*. Shown below are the β-galactosidase activities produced by a translational fusion with the *E. coli fieF* gene in the mutant compared with the wild type (Grass et al., 2005). This gene, although activated by iron concentration, is not *fur* regulated, as shown by the similar expression profiles of *fieF* in wild type and Δ*fur::cat* mutant of *E. coli* in response to increasing iron concentrations. A Fur-responsive gene would be expected to decrease in concentration / activity as iron concentration increased. The Δ*fur::cat* mutant has a higher expression of the iron-responsive *fieF* simply because, in the absence of Fur, the cell will have a somewhat higher intracellular iron content. The increased concentration of the FieF protein would export the excess iron and maintain some homeostasis.

Figure 5.2.2 Heat map of stress response for DVU1778 in *D. vulgaris*. The numbers to the left represent the final concentration of described stressor in the treated cultures and the time of exposure. The colored boxes are coded for the level of differential transcription when compared with an untreated culture at the same growth stage. The column of boxes in the middle is the color key for ratios of transcription of treated cells versus control.

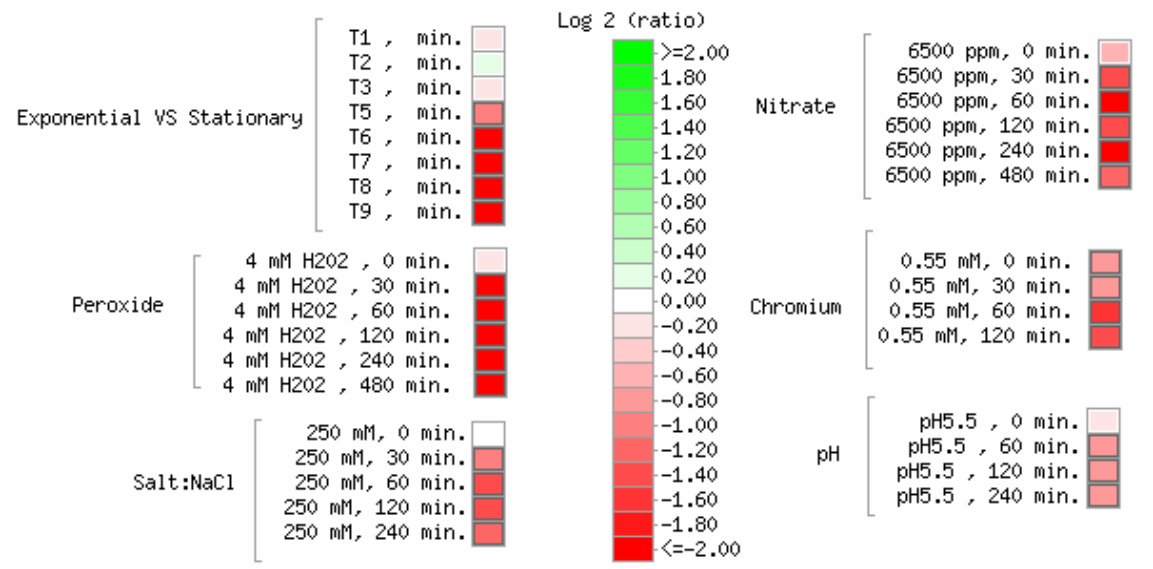
Log 2 (ratio)
>=2.00
1.80
1.60
1.40
1.20
1.00
0.80
0.60
0.40
0.20
0.00
-0.20
-0.40
-0.60
-0.80
-1.00
-1.20
-1.40
-1.60
-1.80
<=-2.00
Exponential VS Stationary
T1 , min.
T2 , min.
T3 , min.
T5 , min.
T6 , min.
T7 , min.
T8 , min.
T9 , min.
Peroxide
4 mM H202 , 0 min.
4 mM H202 , 30 min.
4 mM H202 , 60 min.
4 mM H202 , 120 min.
4 mM H202 , 240 min.
4 mM H202 , 480 min.
Salt:NaCl
250 mM, 0 min.
250 mM, 30 min.
250 mM, 60 min.
250 mM, 120 min.
250 mM, 240 min.
Nitrate
6500 ppm, 0 min.
6500 ppm, 30 min.
6500 ppm, 60 min.
6500 ppm, 120 min.
6500 ppm, 240 min.
6500 ppm, 480 min.
Chromium
0.55 mM, 0 min.
0.55 mM, 30 min.
0.55 mM, 60 min.
0.55 mM, 120 min.
pH
pH5.5 , 0 min.
pH5.5 , 60 min.
pH5.5 , 120 min.
pH5.5 , 240 min.

Figure 5.2.3 *fieF* induction by $FeS0_4$ as measure by a fusion of *lacZ* to the *fieF* promoter region. This graph shows that fieF is not Fur regulated, but regulated by iron concentration. The Δ*fur* has a consistently higher induction of *fieF*, but that is expected considering a higher level of intracellular iron due to the uncapped iron uptake from the deletion of *fur*. If *fieF* were regulated by Fur an exponential curve would be expected in the Δ*fur* strain and not mirroring the slope of the wild type induction of *fieF*. (reproduced from Grass et al., 2005)

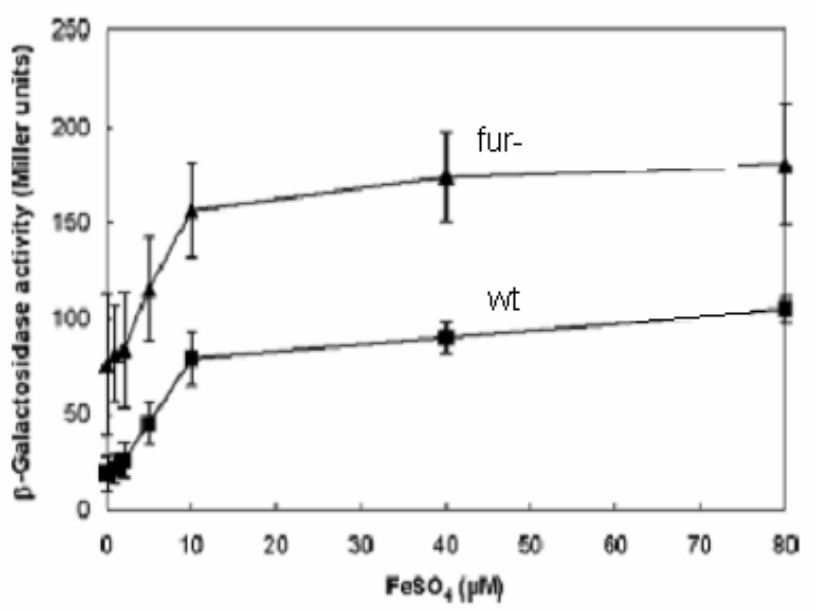
β-Galactosidase activity (Miller units)
250
200
150
100
50
0
fur-
wt
0
10
20
30
40
50
60
70
80
FeSO4 (μM)

Figure 5.2.4 *fieF* is responsible for lower intracellular Fe concentration. The solid squares represent the Δ*fieF* strain that has had FieF complemented by a plasmid copy of the gene, versus the open squares representing a Δ*fieF* strain. The graph shows the *E. coli* strain lacking FieF has an increasingly higher concentration of intracellular iron compared to the same strain with FieF complemented. This is significant evidence that FieF mediates intracellular iron content as an Fe-specific efflux pump. (reproduced from Grass et al., 2005)

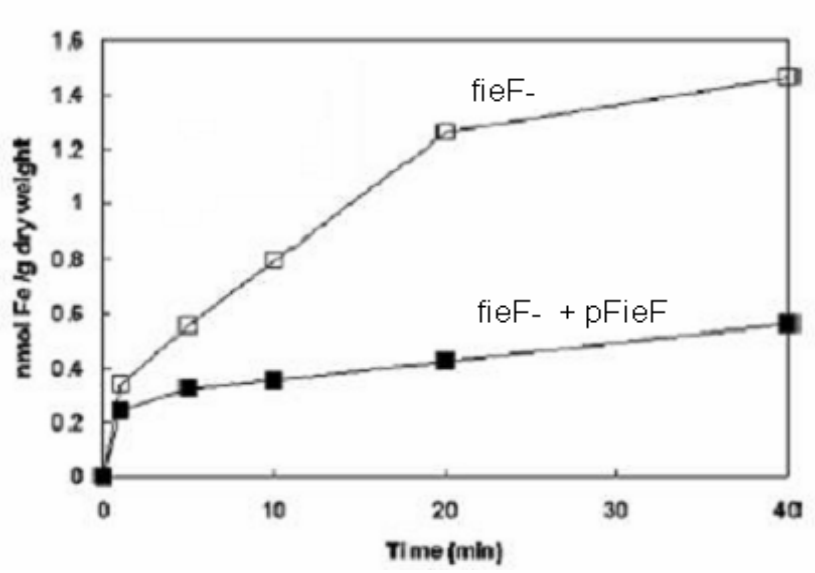
fieF-
fieF- + pFieF
nmol Fe /g dry weight
Time (min)
0
0.2
0.4
0.6
0.8
1
1.2
1.4
1.6
0
10
20
30
40

Deletion of the *D. vulgaris* ortholog for *fieF,* predicted as the first of a two gene operon (MicrobesOnline.org) was unsuccessful, suggesting it may play an essential role in the iron nutrition of this anaerobe. The downstream gene is a putative carbonic anhydrase. It was anticipated that should either of these actually be essential that we would have recovered insertion of the plasmid rather marker exchange. Since this was also not observed, further experimentation is needed to elucidate the inability to obtain the correct construct.

As a control for any technical problems in our efforts to delete *fieF*, attention was turned to another CDF, DVU0164, and it was deleted. This strain was constructed by marker exchange mutagenesis with no apparent difficulties and was designated JW0407. A single 'C' nucleotide deletion was found in the pMO406 mutagenic plasmid located 906 base pairs upstream of the gene in an intergenic region. The distance from any probable promoter and apparent location in a noncoding region reduces the probability of detectable physiological effects resulting from this nucleotide change introduced into JW0407. Strengthening this interpretation was the observation that this deletion strain did not exhibit detectable abnormal growth traits when compared to wild type *D. vulgaris* (data not shown).

Differential growth of this mutant on a complete battery of electron donors and acceptors that supported growth of wild type *D. vulgaris* (Chapter 2.1) revealed no distinguishing phenotypes. In addition, growth at pH 5.5 and fermentative growth were tested and again no discernible growth differences between JW0407 and the wild type *D. vulgaris* were observed (data not shown).

5.4 Efflux Pumps

After studies on the *rnf* operon, other Na^+-dependent transporters became points of interest for phenotypic studies in *D. vulgaris*. Two NorM genes annotated as *norM* paralogs, encoding proteins belonging to the MATE (Multidrug And Toxic compound Efflux) family were annotated in the *D. vulgaris* genome. The two genes, DVU1217 and DVU2555, were deleted by marker exchange, and the deletion strains designated as JW0405 and JW0409, respectively. The predicted operon for DVU2555 (Alm et al., 2005) is shown below, with the downstream gene being a 'conserved hypothetical protein' (Figure 5.3.1). The DVU1217 gene is predicted to be monocistronic. These are the only MATE family antiporters in *D. vulgaris*, although there are other putative antibiotic efflux proteins annotated in the genome including a copy of the *acrAB-tolC* operon. (See below.)

Orthologs of these genes have been studied in *Vibrio parahaemolyticus* (Morita et al., 1998) and proven to encode Na^+-dependent multidrug antiporters. These researchers demonstrated that the proteins had efflux activity for norfloxacin and through complementation of an *E. coli acrAB* mutant showed that this transporter increased resistance to ciprofloxacin, ethidium, kanamycin and streptomycin. The AcrAB complex is the major multidrug efflux system in *E. coli* (Morita et al., 1998).

Figure 5.3.1 Operon prediction for DVU2555, a gene encoding an apparent multidrug efflux pump. Blue filled arrows represent DVU2555 (darker) and DVU2554 (lighter) and the head of the arrow represents the direction of transcription. Numbers are the exact number of nucleotides between predicted genes. White arrows represent genes not part of an operon with DVU2554-DVU2555.


nifU-3
COG4866
COG-NarH
DUF2566
103
-13
147

Complementation of *E. coli* Δ*acrAB* (KAM3 strain; Morita et al., 1998) was accomplished by capturing the PCR products of the putative *D. vulgaris norM* genes, including 300 bp upstream and 100 base pairs downstream of the predicted coding sequences, in pCR-TOPO4 plasmid (Invitrogen, Carlsbad, CA). The up- and downstream ranges of the predicted coding regions were chosen to ensure complementation of any putative promoter and terminator sequences outside the coding regions; along with primer design considerations concerning melting temperature, GC content, and secondary structures. The transformation technique for *E. coli* was identical to that described in Chapter 2.2. The captured gene product was sequenced to ensure no errors were introduced during the PCR procedure. In the presence of the complementing *D. vulgaris norM* gene, either DVU1217 or DVU2555, the *E.coli* Δ*acrAB* strain exhibited an increase in its minimum inhibitory concentration for growth for chemicals such as: ethidium bromide, methylene blue, safranin O, and acridine orange (Fig. 5.3.2 and data not shown).

It was shown (Fig. 5.3.2) that the *E. coli* mutant complemented with DVU1217, a putative *D. vulgaris norM* gene, had increased resistance to the toxic Safranin O compound from 0 μg/ml to 4 μg/ml. The empty vector sample and negative control samples showed no growth over the time duration of the experiment (not shown).

Deletion via marker exchange mutagenesis was performed for both genes in *D. vulgaris*. In JW0405, ΔDVU1217, there were five single base pair mutations in the 55 base pairs downstream of the stop codon. These mutations were not expected to cause

Figure 5.3.2 Two ml LC medium with 20 µl overnight inoculum was present at time zero in each tube. Lanes 1-2 were LC only, Lanes 3-4 had 2 µg/ml Safranin O added, Lanes 5-6 had 4 µg/ml Safranin O added, and Lanes 7-8 had 8 µg/ml Safranin O added. The odd numbered lanes contain the ΔAcrAB *E. coli* mutant and the even numbered lanes contain the ΔAcrAB *E. coli* mutant complemented with DVU1217.

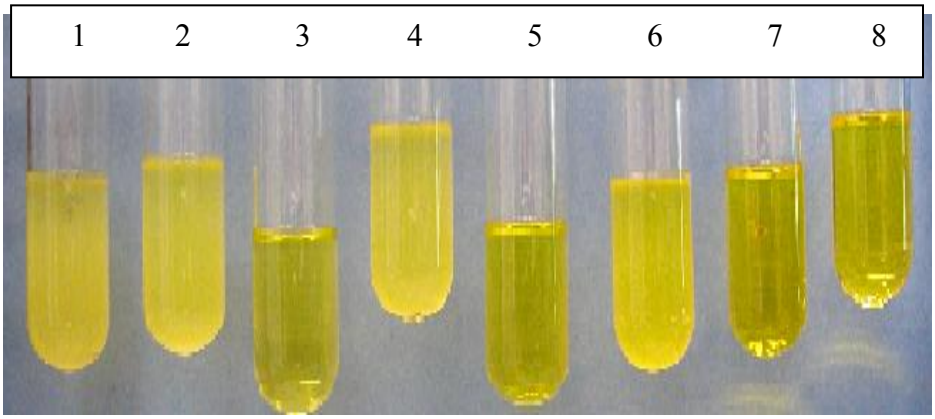
1
2
3
4
5
6
7
8

any phenotypes because they were not in a predicted coding sequence and did not appear to be in a region that might have promoter function. JW0409, ΔDVU2555, had two single nucleotide mutations. The first was a 'G' to 'A' mutation 15 base pairs upstream of the former start codon for DVU2555. The other was a 'A' to 'G' mutation in the downstream conserved hypothetical protein. This latter mutation is silent and does not alter the predicted coded amino acid. Neither of these mutations is predicted to alter the phenotype of the deletion resulting from the marker exchange mutagenesis.

Although growth of *D. vulgaris* with ethanol is quite limited, the mutants JW0405 and JW0409 were both impaired in growth with this substrate and either sulfate or sulfite as the terminal electron acceptor (Figs. 5.3.2 and 5.3.3). Interestingly, no differences between the mutants and wild type were noted when growing on ethanol with thiosulfate as the electron acceptor.

Successful complementation of the *E. coli* mutant lacking multidrug exporters by the *D. vulgaris* NorM genes and impaired growth phenotypes of the *D. vulgaris* Δ*norM* candidates, JW0405 and JW0409, in multiple media supports a role for the mutant sodium-based multidrug exporters in the sodium circuitry of *D. vulgaris* metabolism. Further study detailing the exact role these genes play in the overall physiology could be accomplished through a double marker exchange deletion of these genes and RT-PCR experiments examining expression conditions.

Figure 5.3.3 Ethanol / Sulfate medium; JW0405 (blue), JW0409 (green), and WT (red). The two mutants, JW0405 and JW0409, show a distinct impairment of growth compared to the wild type.

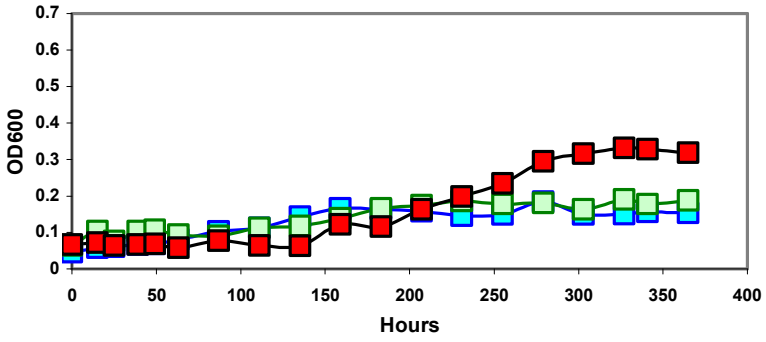
0.7
0.6
0.5
0.4
0.3
0.2
0.1
0
OD600
0
50
100
150
200
250
300
350
400
Hours

Figure 5.3.4 Ethanol / Sulfite medium; JW0405 (blue), JW0409 (green), and WT (red). The mutants, JW0405 and JW0409, show a significant growth lag on ethanol / sulfite medium compared to wild type.

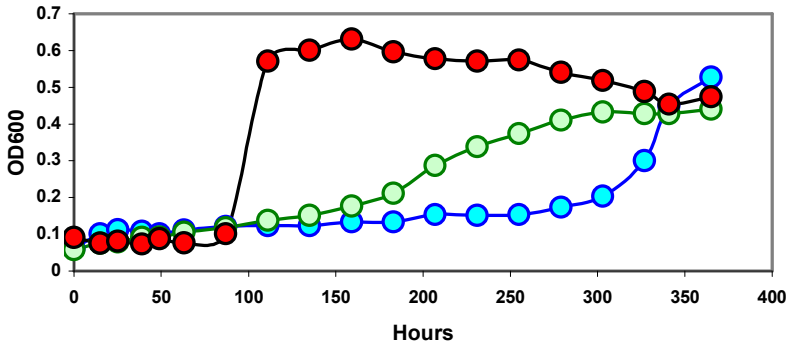
0.7
0.6
0.5
0.4
0.3
0.2
0.1
0
OD600
0
50
100
150
200
250
300
350
400
Hours

5.5 Conclusion

The range of ion transporting genes carries the responsibility for a diverse selection of important physiological capabilities in *D. vulgaris*. The *rnf* operon is Na^+-dependent transporter that was shown to be essential for fixing nitrogen in *D. vulgaris*, confirming the phenotype originally observed in *R. capsulatus* (Jouanneau et al. 1998; Saeki and Kumagai, 1998). In *D. vulgaris*, the CDF family protein, DVU1778, was observed to be encoded by a potential homolog to a gene in *E. coli* that was crucial for removing intracellular iron stress, *fieF* (Grass et al., 2005). Although this gene could not be deleted in *D. vulgaris* some evidence supporting this role was extrapolated from available microarray data. Another CDF, DVU0164, was deleted, although a distinctive phenotype has not been ascertained at the time of this publication. These results were interpreted to mean that the two CDF proteins did not mediate redundant activities in the cell. The two putative *norM* genes in *D. vulgaris*, DVU1217 and DVU2555, were demonstrated via complementation of an *E. coli* mutant to encode proteins that export a variety of toxins. Both were effective in complementation assays with *E. coli* and distinguishing phenotypes have not been identified to date.

All of the systems described here are distinct families of genes encoding cation transporters. With the possible exception of DVU1778 encoding an apparent FieF ortholog, the presence of these genes is not essential for viability of *D. vulgaris* under our standard laboratory conditions. However, they appear to play a role in providing protection under specific stress-inducing conditions.

Chapter 6

SOFTWARE UTILITIES

6.1 Introduction

During my tenure in the Wall lab various projects yielded the potential for useful software utilities to be written that would allow higher throughput methodologies to be adopted, as well as saving man hours. Being able to automate the identification of genomic DNA sequences adjacent to genes targeted for deletion by marker exchange mutants (Bender *et al*., 2007) saved time and allowed for mutants to be constructed more quickly. That was the purpose of "GeneFinder." Secondly, "BLASTFinder" provides quick location of insertion sites of transposons from BLAST results of flanking sequences. This tool has established the basis for high throughput characterization of transposon mutants. With the successful creation of these tools another lab member was stimulated to ask for a utility that would automate the selection of restriction endonucleases for genomic digests for Southern Blots. I then generated "Restriction Mapper" for that purpose. Finally, I addressed the problem of disparate gene nomenclature for *D. vulgaris* annotated genes in available databases. Lists were generated, "Master Lists" to have a concise table of all necessary information about the SRB genomes and easily translate from various naming conventions to avoid the difficulties of multiple designations for a single gene. The following sections detail the construction of these various programs and serve as a 'Help' section for these utilities.

6.2 GeneFinder

The utilities available at http://www.microbesonline.org/ display only the protein coding sequences and translated proteins, along with other annotation information.

Recent modifications to the MicrobesOnline.org site have improved sequence accessibility, but the up- and downstream sequences available for each ORF are still restricted to 250 bp. The information contained at this site was not sufficient to design the necessary experiments required to construct marker exchange mutants. Hence, a program was written to facilitate location of the intergenic regions in the genomic sequences of the *Desulfovibrio* strains and constructs of interest in the Wall lab.

The need for easy access to intergenic DNA sequences up- and downstream of target genes became apparent when primers were being designed for the construction of marker exchange mutants (see Chapter 2.3.1 for details). For the deletions, about 1000 bp up- and downstream of the gene targeted are cloned on either side of the selectable antibiotic resistance gene. With only a file containing the complete genome sequence and ORF sequences available, the methodology available for accessing the sequences surrounding ORFs was very tedious and time consuming and needed to be repeated for every set of primers associated with the creation of a mutant. The complete genome sequence had to be manually searched for the position of the targeted gene, this was a not a trivial task considering the size of the genome and the limited search mechanisms available in most word processing software, it was even more difficult for genes encoded on the opposite strand of given genome sequence file. Upstream, downstream, and coding regions had to be identified before potential primers could be identified. Therefore the following search protocol was developed (Fig. 6.2.1).

Figure 6.2.1 Input options for GeneFinder.

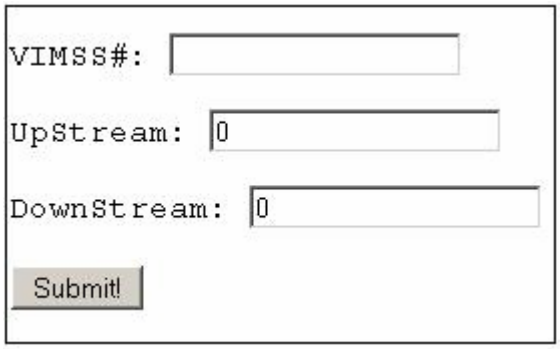
VIMSS#:
UpStream: 0
DownStream: 0
Submit!

The input options (Fig. 6.2.1) are streamlined and efficient. The 'VIMSS#' is a six digit unique identifier for each putative gene assigned from the MicrobesOnline.org website. The upstream and downstream boxes are for identifying how many DNA base pairs are desired to be shown before the annotated start codon of the target ORF and following the stop codon, respectively. Clicking the 'Submit!' button provides the results for the given gene and intergenic regions. An example is given in Fig. 6.2.2 (output is shown in Figs. 6.2.3 and 6.2.4).

The inputs are verified and then processed. All genes in the genome are listed in a lookup table. That table contains a listing of the gene's VIMSS#, two numbers designating the base pair within the genome where the gene starts and ends, and a '+' or '-' signifying the strand on which the gene is located. The program locates the input gene within the lookup table. The offsets are calculated in accordance with the 'UpStream' and 'DownStream' numbers provided. The region of sequence is located within the genome sequence file and extracted.

The sequence output is in lines of 60 base pairs with the gene colored in red and the intergenic regions, or simply DNA regions up- and downstream of the target gene, in black. If the gene is on the negative strand, the reverse complement is supplied so the sequence given is the sense strand of the gene. These notifications are provided above the sequence, including a link to the MicrobesOnline.org page supplying other information about the gene (Fig. 6.2.3 below).

Figure 6.2.2 Input example for GeneFinder.

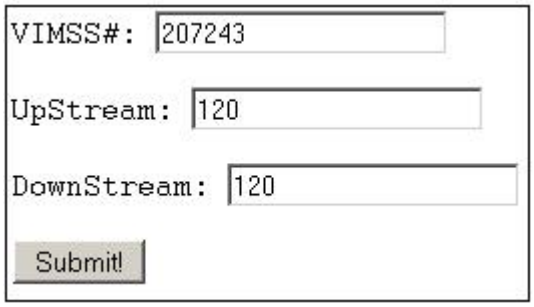
VIMSS#: 207243
UpStream: 120
DownStream: 120
Submit!

Figure 6.2.3 Output example for GeneFinder.

VIMSS207243
The gene is on the main chromosome.
Gene Requested is on the Minus (-) Strand.
The reverse complement is provided below.

Figure 6.2.4 Sequence output from GeneFinder.

GATGTCGATGCCATCAGCAGGTGAACTGCCCGCAGGCATTGGCCTCGTAGCCGCGACATG
GGGGTGAGCGGCTTGCCTCGTGCGCGCCGCCGCCGGATGCCAGATTCTACCGGAGTGAGC
ATGTCAGACGATTATACCTATATCGCCGAGGCCGACAGGGAGAAGCGCATCGCTGCGCTT
TCATCCGTCGGGGCGGCTTTGCTGCTTACGGGACTCAAACTGGGAGTGGGGTTCGCCACC
AACAGTCTGGGCATCCTCTCCGAAGCGGCCCATAGCGGTCTCGACCTTGTTGCCGCGGTC
GTGACCTACTGGGCTGTTCGTGCGGCGTCGCGCCCCGCCGATGCCGACCATCCCTACGGG
CACGGCAAGGTGGAGAACCTCTCCGCGCTTGTGGAGACGTTACTGCTGTTGCTCACCTGC
GGCTGGATTGTGCGTGAAGCCGTCGACAGACTCTTCTTCGAAGCCGTTCATGTGGAACCT
TCGGTATGGGGGCTTGCCGTCATGGGCGTCTCAATCGTCGTCGACATTTCCCGTGCACGC
ATGCTGCGCCGGGTCGCCCGCAAGCACAACAGTCAGGCACTGGAAGCCGACGCCCTGCAT
TTCTCGACGGACGTATGGTCTTCGGCGGTGGTCATCGCGGGGCTTCTGGCGTTGCGCGCC
GCCATGTTCTTTCCGCAGGACTCGTTCATGTTCGCCGTGCTGCAACGGGCTGATGCCTTC
GCGGCACTCGTCGTGTCGTGCATCGTCGTTTTCGTGAGCCTGCAACTTGGTCGACGCGCT
GTCGACGTGCTGCTCGACGGCGGGGCGCAGGAACAGGTCGAGCGTGCTGCGGATGCCCTG
AAGGATTTGCCGGGTATCGTCCGCATCGAGCGACTTCGGGTACGCCAGAGTGGGCCTCGC
ACATTTGTCGACCTGTTGCTTTGCGTGCCGCAAGGGATGAGCTTTGAAGCGTCTCATACT
CTTTCCGAACAGGCCGAACGCCGTCTCCAGGCGGTGCTTCCCCAAGCCGACGTTATCGTA
CACATGGAACCCGCCAGTCCCGACGAGGTGGGGATGCTCGAACGTATCCGTGGTGTTGCC
GCTTCACACGGGCTTGCCGTGCATGCCGTTTCGTTCATGCTGGTCGACGGAGAACAGCAT
GTCGACCTGCATGCAGAGGTCGCCGGAGAGGAACGGCTTGAAGTCGCGCATGAGCGGGTG
AGTGCGTTCGAAGCCGACCTTGCGAGAACGCTGGGCAAAGCCACGGTGGTGACGCATATC
GAACCGGTCGCTGTTCGCGAGGATGCCCTGCCGGAGGCAAGTAATGAGGCGCTCACTGCT
GTGGAAGGGGTGGTGCACTCCCTGCTTGACGCAGAGCCTGACGTCGACGATTGTCACAAC
ATGCGGCTTCACCGGCTAGGTGATGAGCTTTCGTTGAGCTTTCATTGCCGCATGTCTCCC
GAAACCCCGGTGTCGGTCGCCCATGAGGCCGCTACGCGACTTGAGAAGTCCCTGCGTGCA
AGGTTGGGTGATATCTCTCGGGTGGCCATTCATATGGAGCCGACGCCGCGAAACCATCAG
GCTTAACGATCAGGACAGAGGACATTCGATGCCACAGAGGGATCTCGACAGGTTCATCGC
CGGTTTTCGCCGGTTTCAGCGTAACTATTTTTGCCACGACCACAATCTGTTCGAATCCTT
GCGTGA

There are currently versions of GeneFinder for *Desulfovibrio vulgaris* Hildenborough and *Desulfovibrio desulfuricans* G20. These two strains are both being used as model organisms to attempt to delete or mutate every gene systematically.

6.3 BLASTFinder

A program was written to aid in mapping the location of insertions of Tn5-RL27 transposon (Larson et al., 2002) following random mutagenesis of *D. vulgaris* (see Chapter 2.4 for details). This program has also been used as tool to obtain locations and extents of genomic DNA fragments captured in a plasmid library.

A library of over five thousand Tn5-pRL27 mutants has been constructed in *Desulfovibrio vulgaris* Hildenborough (J. Ringbauer and J. Wall, unpublished). Direct sequencing from chromosomal DNA adjacent to the transposon from a primer with homology to the transposon sequence was unsuccessful for the identification of the site of insertion. An alternative procedure, a nested semi-random PCR procedure (Chun et al, 1997) was subsequently productive in amplifying the DNA regions flanking the transposon (M. Shirley and J. Wall, unpublished). The amplicons were sequenced; the sequences of the flanking regions were then located on the sequenced genome, and if appropriate, correlated to a given ORF.

The BLAST (Basic Local Alignment Search Tool) was used to locate the base pair number of the sequence flanking a transposon by alignment of the amplicon sequence with the genome (Fig. 6.3.1). The standard BLAST output has no way of locating or identifying the gene or intergenic region matching the query sequence. It only designates a single number that cryptically corresponds to a location on the chromosome.

Figure 6.3.1 Example BLAST output.

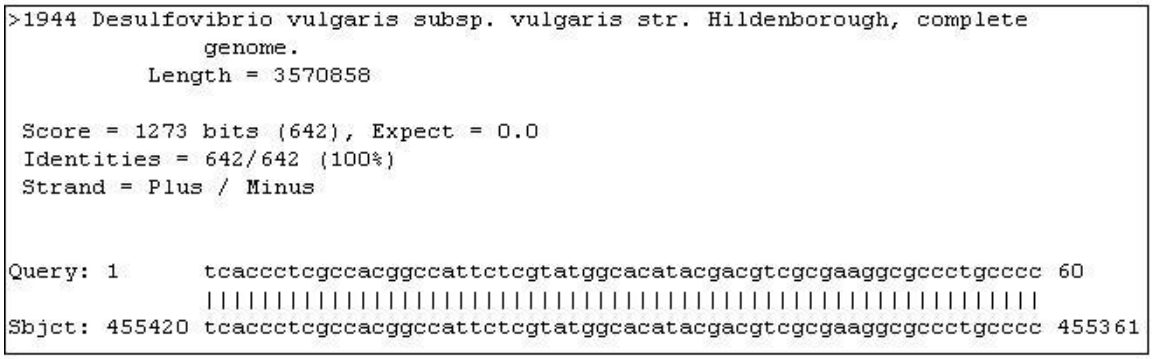

```
>1944 Desulfovibrio vulgaris subsp. vulgaris str. Hildenborough, complete
             genome.
          Length = 3570858

 Score = 1273 bits (642), Expect = 0.0
 Identities = 642/642 (100%)
 Strand = Plus / Minus


Query: 1       tcaccctcgccacggccattctcgtatggcacatacgacgtcgcgaaggcgccctgcccc 60
                ||||||||||||||||||||||||||||||||||||||||||||||||||||||||||||
Sbjct: 455420 tcaccctcgccacggccattctcgtatggcacatacgacgtcgcgaaggcgccctgcccc 455361
```

The tool I developed uses the number returned by BLAST to identify the genetic location of the transposon. The number identifying the first base of the sequence matching the query sequence is typed into the BLASTFinder box (BP; Figure 6.3.2). The lookup table described for GeneFinder is searched for the ORF with coordinates closest to the query for base pair, 'BP'. The closest gene is given, along with a link to the MicrobesOnline.org page containing the gene description (MicrobesOnline.org) and an exact location of the base pair in relation to the N- or C-terminus of the gene (Fig. 6.3.3).

At present, BLASTFinder has only been established for *D. vulgaris* Hildenborough, although it is easily adaptable for *D. desulfuricans* G20 if the need arises. Approximately 100 Tn5-RL27 mutants have been sequenced thus far by the Wall lab using this tool for determining the transposon integration site.

6.4 Restriction Mapper

Tagging genes for visualization of the encoded protein, for locating the final protein product within the cell, and isolating the protein by immunoprecipitation to ascertain protein complexes is a powerful genetic tool being applied by the Wall lab. A useful confirmation of the successful tagging of genes in *D. vulgaris* Hildenborough involves Southern analysis of genomic DNA restriction fragments from the parental wild type cells and the tagged constructs. The tagged constructs have the tagging vector integrated into the chromosome and two copies of the target gene are present (Fig. 6.3.1). Southern analysis of digested genomic DNAs of the construct versus the WT strain will reveal whether the tagging vector has integrated into the chromosome generating a partial diploid for the cloned sequences. An unambiguous pattern of DNA bands is needed to

Figure 6.3.2.Input box for BLASTFinder, ‘BP’ stands for Base Pair that will be located within the genome of *D. vulgaris* and described in context of proximity to a predicted gene shown in Fig. 6.3.3.


BP : 941980
Submit!

Figure 6.3.3 Output example from data used in Fig. 6.3.2.

That position is within gene: VIMSS206279
It is 480 bp from the N-terminus.

distinguish the wild type chromosomal structure from that generated following vector integration. This requires knowledge of the potential DNA fragment sizes produced by the restriction endonuclease used for genomic DNA digestion. Because the fragment patterns of several endonucleases were often needed before an interpretable pattern was obtained, prediction of the expected DNA restriction endonuclease fragment sizes was very tiresome and could be streamlined and automated. Hence, this tool was created.

Upon integration of the tagging vector there should be two copies of the gene; the tagged copy of the gene would remain regulated by the wild-type promoter, while the secondary copy would remain untagged and might not have a promoter. An example for the *dsrC* gene (VIMSS# 208282 / DVU# 2776) is provided in Fig. 6.4.1.

A utility was created that accepts the VIMSS six digit identifier unique to each gene, the orientation of the tagged gene sequences captured in the tagging vector (revealed when the cloned gene is sequenced in the tagging vector), and the tag used in the construct (Fig. 6.4.2).

To make the comparison simple, restriction endonucleases that do not cut the wild type target gene were selected. Therefore, a single band would be revealed in the Southern for the wild-type and two bands would be seen in a successfully tagged construct probed with a fragment internal to the target gene if the vector contained at least one cut site. A list of all restriction endonucleases that cut the sequence in the required three places (upstream, downstream, within the plasmid) and do not cut within the gene are listed. Also given are the fragment sizes for the two bands (the tagged copy of the gene and the untagged copy) in the construct and the size of the fragment in the

Figure 6.4.1 Map of *Sph*I digest genomic DNA in the region of *dsrC* and the tagged construct. The wild type genome cut with SphI would generate a 5589 bp fragment containing the *dsrC* gene. By comparison, *dsrC* would be found on two fragments of 6958 and 3145 bp if the tagging vector had successfully integrated in the correct position of the chromosome. These fragments are readily distinguishable when probed with *dsrC* in Southern blot analysis.

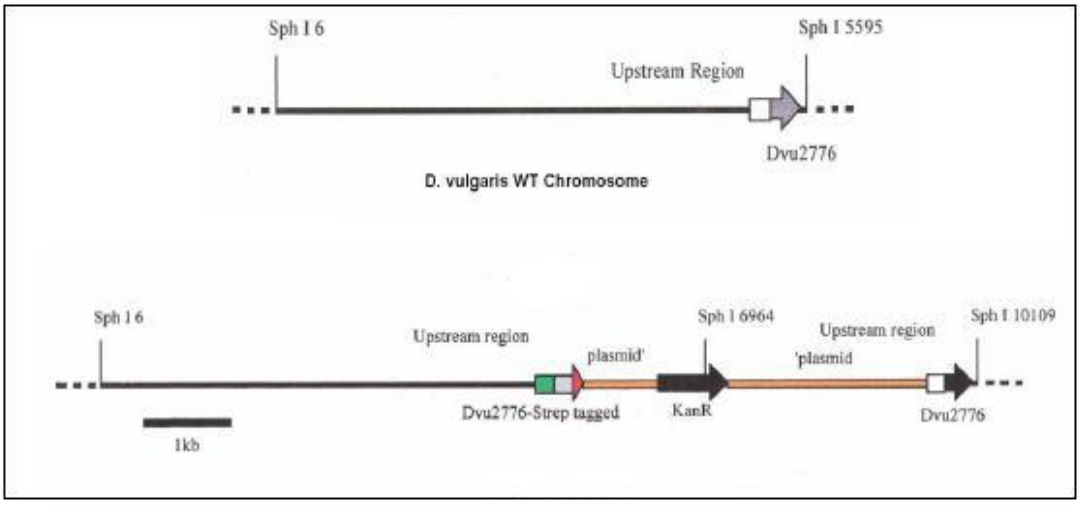
Sph I 6
Sph I 5595
Upstream Region
Dvu2776
D. vulgaris WT Chromosome
Sph I 6
Upstream region
plasmid'
Sph I 6964
Upstream region
'plasmid
Sph I 10109
Dvu2776-Strep tagged
KanR
Dvu2776
1kb

Figure 6.4.2 Input options for Restriction Mapper.

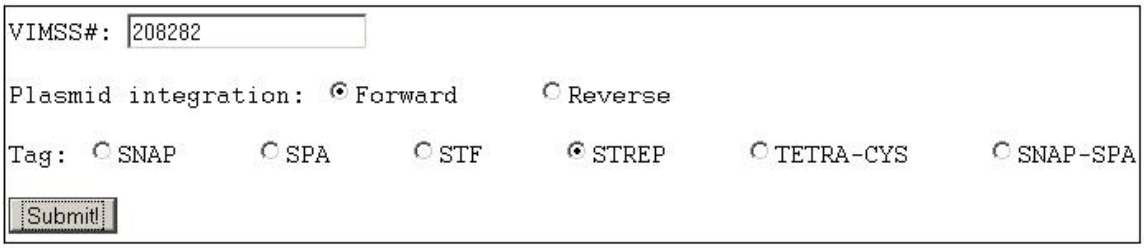
VIMSS#: 208282
Plasmid integration: Forward Reverse
Tag: SNAP SPA STF STREP TETRA-CYS SNAP-SPA
Submit!

Figure 6.4.3 Restriction enzymes and band sizes. The two copies of the tagging construct are referred to as “Tagged Gene” and “Untagged Gene.”

```
PvuII**************************
Cut sequence : CAGCTG
Tagged Gene Size = 562
UnTagged Gene Size = 757
WT Gene Size = 588

SphI**************************
Cut sequence : GCATGC
Tagged Gene Size = 6955
UnTagged Gene Size = 2935
WT Gene Size = 5588

Tsp509I**************************
Cut sequence : AATT
Tagged Gene Size = 594
UnTagged Gene Size = 1572
WT Gene Size = 1802
```

wild-type control. All restriction endonucleases that meet the criteria are printed so those with the most easily distinguishable band sizes could be identified and a correlation made with the enzymes available. Of course, the tagging vector and its sequence must be known. For the example given here, pCR®4Blunt-TOPO® (Invitrogen, Calsbad, CA).

An ideal banding pattern would look similar to Fig. 6.4.4, with distinct band sizes for the 'WT' control lane and the experimental lanes '521-2776' and '965-2776-1'. The probe used was an internal fragment of the gene tagged.

In addition to the restriction enzymes and fragment sizes, the fully assembled sequence is provided. This sequence is the modified genome after insertion of the tagging vector, as shown in Figure 6.4.1. This sequence includes 8000 base pairs up- and downstream of the target gene, is printed according to the color coding in Fig. 6.4.5 in lines of 60 base pairs.

This tool has been updated to include options for more tags and different tagging vectors. This is a very simple process that will allow any future tagging vectors to be added to this tool. It also contains the ability to select either the VIMSS# (old) or enter in the base pair range on the chromosome to include upstream region (new). This was necessary because many constructs have to be designed to include the upstream promoter region of the gene to be tagged, so the gene sequence itself was not enough information to generate an exact map of the construct upon integration of the plasmid and the predicted Southern blot fragments did not correlate with the fragment sizes obtained.

Figure 6.4.4 Southern blot film. Distinct band sizes for the ‘WT’ control lane and two bands, one larger and one smaller that the ‘WT’ control lane, are shown in the experimental lanes ‘521-2776’ and ‘965-2776-1’. The probe used was an internal fragment of the tagged gene.

0
1cm
2
3
4
5
6
7
8
9

Figure 6.4.5 Output color codes and total size of sequence listed. Note: Some sequence has been trimmed to save space.

Gene Coding Sequence
Tag Sequence
Topo4 Plasmid Sequence
NonCoding Genomic Sequence

Total Sequence Size (bp): 20619

TGTCGCGCTTTCATGGTGGCACCGCTCACAGGGTACTGCATAGTCTGCGGCGTGTTTCTT
GTGGTCGAACACCACCTTGCCACCTGCGTTGTCGAATCGGATGCGCGTCGGAACGGCTCC
GGCCACGTCTCCTGGTATTGAATAACCAAACAACGCGACAATTGCCATCAGTCCAGTGAA
CACAACAACGGAGATGTAGCGTTTGGGCATGGCCAACCTTCATCAATGAGAAGTTACAAC
GATGCACTCCTGACGAACTTTTGCATGGACATTGGCATGTTGTGAGGGTTTTGGAAAGTG
ATGGGCTGTATTTTCTAAAAGAACATTATTTCACAAGCCTTGCACTCGGTTGCGGAGAAA
ACCCGGGTAAGTGGCGTAATCCTTGTGAATGCATCGTATAGTGGAGCCACCCGCAGTTCG
AAAAATAAAAGGGCGAATTCGCGGCCGCTAAATTCAATTCGCCCTATAGTGAGTCGTATT
ACAATTCACTGGCCGTCGTTTTACAACGTCGTGACTGGGAAAACCCTGGCGTTACCCAAC
TTAATCGCCTTGCAGCACATCCCCCTTTCGCCAGCTGGCGTAATAGCGAAGAGGCCCGCA
CCGATCGCCCTTCCCAACAGTTGCGCAGCCTATACGTACGGCAGTTTAAGGTTTACACCT
GAAGCGGAAGAGCGCCCAATACGCAAACCGCCTCTCCCCGCGCGTTGGCCGATTCATTAA
TGCAGCTGGCACGACAGGTTTCCCGACTGGAAAGCGGGCAGTGAGCGCAACGCAATTAAT
GTGAGTTAGCTCACTCATTAGGCACCCCAGGCTTTACACTTTATGCTTCCGGCTCGTATG
TTGTGTGGAATTGTGAGCGGATAACAATTTCACACAGGAAACAGCTATGACCATGATTAC
GCCAAGCTCAGAATTAACCCTCACTAAAGGGACTAGTCCTGCAGGTTTAAACGAATTCGC
CCTTTTGCATGGACATTGGCATGTTGTGAGGGTTTTGGAAAGTGATGGGCTGTATTTTCT
AAAAGAACATTATTTCACAAGCCTTGCACTCGGTTGCGGAGAAAACCCGGGTAAGTGGCG
TAATCCTTGTGAATGCATCGTATAGGCAAGCGCAAGGCCTTGAGAAGACTGCATTCGGAG
TCGACTGGTTCATTTTTCCCGCGACGAAGTGCGAGACAGGCGTTCTGTATTTATGCAACG
GGTTCTAGGGGGACAGTCGAAGCCACACTGCCGGTATCGGGACGAATACATCAATGAACC
GGAATGGTATGCAATAAAAAATGCAGTGTGCTGTGCGTCCTGCACTGTGTGAGCGCACAG

6.5 Lists

After obtaining the full genome sequence (Heidelberg et al. 2004; http://genome.ornl.gov/microbial/ddes/2005) of the sulfate reducers studied in the Wall lab, an issue arose of consistent naming of the genes. An initial assignment of putative ORFs (Open Reading Frames) was made either at The Institute for Genome Research (http://www.tigr.org/) or the Joint Genome Institute (http://www.jgi.doe.gov/). Then annotation resulted in functional names (such as *dsrC* or *rnfC*) for a large portion of the ORFs. Further, new designations were made by other groups and by NCBI. Finally, MicrobesOnline.org assigned a unique identifier for each gene. With different groups using different designations for genes it was beneficial to have a master list to facilitate cross referencing of the various naming schemes.

6.5.1 *Desulfovibrio vulgaris* Hildenborough Master List

A program was designed to pull information from the MicrobesOnline.org site. This included the VIMSS#, DVU#, ORF#, name, description, COG, strand, and base pair coordinates. This was then parsed out of the raw data pulled from the web and formatted. These data were then ordered and put in a spreadsheet. This accessible list was also very useful to have while analyzing the microarray data for stress responses (Chapter 3) and establishing the validity of hypothetical genes (Chapter 4). An example of a short region of the master list for *D. vulgaris* Hildenborough is given in Figure 6.5.1.

Table 6.5.1.1 Segment of *Desulfovibrio vulgaris* Hildenborough Master List table (some columns condensed for page space concerns).

VIMSS#	Name	DVU#	ORF#	Description	COG	Start	End	Strand
VIMSS208998	yhaO	DVU0070	ORF04748	Ser/Thr protein phosphat	COG420, DNA repair exonuc	85666	87021	-
VIMSS208999	dinP	DVU0071	ORF04749	DNA polymerase IV (TIG	COG389, Nucleotidyltransfer	87539	88699	+
VIMSS209000	mpg	DVU0072	ORF04750	glucose-1-phosphate cyt	COG1208, Nucleoside-dipho-	89105	89884	+
VIMSS209001		DVU0073	ORF04751	CDP-glucose-4,6-dehydr	COG451, Nucleoside-diphos	89894	91000	+
VIMSS209002		DVU0074	ORF04753	polysaccharide biosynth	COG1898, dTDP-4-dehydrh	90988	91431	+
VIMSS209003	rfbE	DVU0075	ORF04754	aminotransferase, DegT/	COG399, Predicted pyridoxa	91765	92898	+
VIMSS209004		DVU0076	ORF04756	glycosyl transferase, gro	COG463, Glycosyltransferas	92949	93953	+
VIMSS209005		DVU0077	ORF04757	conserved hypothetical p	COG4129, Predicted membr	94316	95398	+
VIMSS209006		DVU0078	ORF04759	conserved hypothetical p	COG4095, Uncharacterized	95445	95786	+
VIMSS209007	gufA	DVU0079	ORF04760	ZIP zinc transporter fami	COG428, Predicted divalent	96159	96962	+
VIMSS209008	fumC	DVU0080	ORF04762	fumarate hydratase, clas	COG114, Fumarase [Energy	97000	98406	+

6.5.2 *Desulfovibrio desulfuricans* G20 Master List

The master list of ORFs for G20 was slightly more complicated. The information had to be collected from multiple websites before being correlated. Data were mined from the necessary websites: NCBI, MicrobesOnline.org, and the DOE Joint Genome Institute.

The protein sequence from MicrobesOnline.org (not that it matters which one was used to start) was utilized in the BLAST program against the protein sequences collected from the other sites. This allowed the naming/numbering systems to be matched and thus all the schemes were correlated. An example of a short region of the master list for *D. desulfuricans* G20 is given in Fig. 6.5.2.

Table 6.5.2.1 Segment of *Desulfovibrio desulfuricans* G20 Master List table (some columns condensed for page space concerns).

VIMSS#	Name	Description	Start	End		Dde#	Dde Start	Dde End		NCBI # and Description
VIMSS392913	murA	UDP-N-acetylglucosamine 1-c	117811	119061	-	Dde0546	560473	561723	+	gb|ABB37347.1| UDP-N-acetylgluc
VIMSS392914	barA	Sensor-regulator, activates Or	119554	122499	-	Dde0544	557035	559980	+	gb|ABB37345.1| periplasmic sens
VIMSS392915	mviN	Integral membrane protein Mvi	122606	124189	-	Dde0543	555345	556928	+	gb|ABB37344.1| integral membran
VIMSS392916	mutM	Formamidopyrimidine-DNA gly	124204	125091	-	Dde0542	554443	555330	+	gb|ABB37343.1| formamidopyrimid
VIMSS392917		PDZ domain (Also known as D	125376	126764	-	Dde0541	552770	554158	+	gb|ABB37342.1| PDZ/DHR/GLGF [
VIMSS392918		Coenzyme F390 synthetase fa	126755	128020	-	Dde0540	551514	552779	+	gb|ABB37341.1| phenylacetate-coe
VIMSS392919		Conserved hypothetical protein	128237	129157	-	Dde0539	550377	551297	+	gb|ABB37340.1| protein-L-isoaspar
VIMSS392920		Conserved hypothetical protein	129349	130338	+	Dde0538	549196	550185	-	gb|ABB37339.1| radical SAM doma
VIMSS392921	rne	Ribonuclease E (rne) (VIMSS-	130402	131862	+	Dde0537	547672	549132	-	gb|ABB37338.1| ribonuclease, Rne
VIMSS392922		Uncharacterized BCR, COG16	131865	132521	+	Dde0537	547672	549132	-	gb|ABB37338.1| ribonuclease, Rne

6.6

Conclusion

The software described above is just a fraction of the ideas and potential for automation and significant time savings through software development. Another useful program to be implemented for high throughput transposon mapping would be a searchable database to track sequencing runs, insertion sites, and other pertinent information for each mutant. Continued development for "GeneFinder" would yield automated primer selection for the chromosome fragments that make up the marker exchange vector. The utilities already developed, and those yet to be created, pay for the cost of development within months from the date of deployment through time savings and increased productivity of the scientists using them to aid them in their research. Embracing software involvement within the realm of basic research is a necessity to thrive in the increasingly competitive race for funding and breakthrough discoveries.

Chapter 7

REFERENCES

Allen, T.D., Kraus, P.F., Lawson, P.A., Drake, G.R., Balkwill, D.L., and Tanner, R.S. 2008. *Desulfovibrio carbinoliphilus* sp. nov., a benzyl alcohol-oxidizing, sulfate reducing bacterium isolated from a gas condensate-contaminated aquifer. *International Journal of Systematic and Evolutionary Microbio*. 58: 1313-1317.

Alm, E.J., K.H. Huang, M.N. Price, R.P. Koche, K. Keller, I.L. Dubchak, and A.P. Arkin. 2005. The microbesonline web site for comparative genomics. *Genome Research*. 15: 1015-1022.

Badziong, W. & Thauer, R. K. 1978. Growth yields and growth rates of *Desulfovibrio vulgaris* (Marburg) growing on hydrogen plus sulphate and hydrogen plus thiosulphate as sole energy sources. *Arch. Microbiol.* 117, 209–214.

Barton, L.L. and W.A. Hamilton. 2007. Sulphate-reducing bacteria: environmental and engineered systems. Cambridge University Press, Cambridge.

Beijerinkck, M.W. 1895. Uber *Spirillum desulfuricans* als Urasche von Sulfatreduktion. *Zentralbl Bakteriol Parasitkd Infekt Abt II*. 1: 49-59.

Bender, K.S., H.C. Yen, C.L. Hemme, Z. Yang, Z. He, Q. He, J. Zhou, K.H. Huang, E.J. Alm, T.C. Hazen, A.P. Arkin, and J.D. Wall. 2007. Analysis of a ferric uptake regulator (Fur) mutant of *Desulfovibrio vulgaris* Hildenborough. *Applied and Environmental Microbiology.* 73: 5389-5400.

Bottcher, M. E., Thamdrup, B., Gehre, M., and Theune, A. 2005. S34/S32 and O18/O16 fractionation during sulphur disproportionation by *Desulfobulbus propionicus. Geomicrobiol. J*. 22: 219–226.

Brandis, A., and R. K. Thauer. 1981. Growth of *Desulfovibrio* species on hydrogen and sulfate as sole energy source. *Journal of General Microbiology*. 12**:** 249-252.

Brandis-Heep, A., Gebhardt, N. A., Thauer, R. K., Widdel, F., and Pfennig, N. 1983. Anaerobic acetate oxidation to CO2 by *Desulfobacter postgatei*. *Arch. Microbiol*. 136: 222–229.

Chun, K.T., H.J. Edenberg, M.R. Kelley, M.G. Goebl. 1997. Rapid Amplification of Uncharacterized Transposon-tagged DNA Sequences from Genomic DNA. *Yeast.* 13: 233-240.

Clark, M.E., Q. He, Z. He, E.J. Alm, K.H. Huang, T.C. Hazen, A.P. Arkin, J.D. Wall, J. Zhou, and M.W. Fields. 2006. Temporal transcriptomic analyses of*Desulfovibrio*

vulgaris Hildenborough during electron donor depletion. *Appl. Environ. Microbiol.* 72:5578-5588.

Clark, M.E., Edelmann, R.E., Duley, M.L., Wall, J.D., and Fields, M.W. 2007. Biofilm formation in *Desulfovibrio vulgaris* Hildenborough is dependent upon protein filaments. *Environ. Microbiol.* 9: 2844:2854.

Dudoit, S., and J. Fridlyand. 2002. A prediction-based resampling method for estimating the number of clusters in a dataset. *Genome Biol*. 3**:** 0036.1-0036.21.

Durbin, P.W., B. Kullgren, J. Xu, K.N. Raymond. 1997. New agents for in vivo chelation of uranium (VI): efficacy and toxicity in mice of multidentate catecholate and hydroxypyridinonate ligands. *Health Physcs*. 72: 865-879.

Elias, D.A., Drury, E.C., Redding, A.M., Mukhopadyay, A., Yen, H.B., Fields, M.W., Hazen, T.C., Arkin, A.P., Keasling, J.D., and Wall, J.D. In press. Expression profiling of hypothetical genes in *Desulfovibrio vulgaris* leads to improved functional annotation. *Nucleic Acids Research.*

Fields, M.W., Yan, T., Rhee, S.K., Carroll, S.L., Jardine, P.M., Watson, D.B., Criddle, C.S., and Zhou, J. 2005. Impacts on microbial communities and cultivable isolates from groundwater contaminates with high levels of nitric acid-uranium waste. *Microbial Ecol.* 53: 417-428.

Giaever, G., A. M. Chu, L. Ni, C. Connelly, L. Riles, S. Veronneau, S. Dow, A. Lucau-Danila, K. Anderson, B. Andre, A. P. Arkin, A. Astromoff, M. El-Bakkoury, R. Bangham, R. Benito, S. Brachat, S. Campanaro, M. Curtiss, K. Davis, A. Deutschbauer, K. D. Entian, P. Flaherty, F. Foury, D. J. Garfinkel, M. Gerstein, D. Gotte, U. Guldener, J. H. Hegemann, S. Hempel, Z. Herman, D. F. Jaramillo, D. E. Kelly, S. L. Kelly, P. Kotter, D. LaBonte, D. C. Lamb, N. Lan, H. Liang, H. Liao, L. Liu, C. Luo, M. Lussier, R. Mao, P. Menard, S. L. Ooi, J. L. Revuelta, C. J. Roberts, M. Rose, P. Ross-Macdonald, B. Scherens, G. Schimmack, B. Shafer, D. D. Shoemaker, S. Sookhai-Mahadeo, R. K. Storms, J. N. Strathern, G. Valle, M. Voet, G. Volckaert, C. Y. Wang, T. R. Ward, J. Wilhelmy, E. A. Winzeler, Y. Yang, G. Yen, E. Youngman, K. Yu, H. Bussey, J. D. Boeke, M. Snyder, P. Philippsen, R. W. Davis, and M. Johnston. 2002. Functional profiling of the *Saccharomyces cerevisiae* genome. *Nature*. 418: 387-391.

Gibson, G.R. 1990. A review: physiology and ecology of the sulfate-reducing bacteria. *Journal of Applied Bacteriology*. 769:797.

Grass, G., M. Otto, B. Fricke, C.J. Haney, C. Rensing, D.H. Nies, and D. Munkelt. 2005. FieF (YiiP) from *Escherichia coli* mediates decreased cellular accumulation of iron and relieves iron stress. *Archives of Microbiology.* 183: 9-18.

Greene, E.A., Hubert, C., Nemati, M., Jenneman, G.E., and Voordouw, G. 2003. Nitrite reductase activity of sulfate-reducing bacteria prevents their inhibition by nitrate-reducing sulfide-oxidizing bacteria. *Environmental Microbiology.* 5: 607-617.

Hansen, T.A. 1994. Metabolism of sulphate-reducing prokaryotes. *Antonie Van Leeuwenhoek International Journal of General and Molecular Microbiology*. 66: 165-185.

Haveman, S.A., Greene, E.A., Stilwell, C.P., Voordouw, J.K., and Voordouw, G. 2004. Physiological and gene expression analysis of inhibition of *Desulfovibrio vulgaris* Hildenborough by nitrite. J*ournal of Bacteriology.* 186: 7944-7950.

Hayashi, M., Nakayama, Y., and Unemoto, T. 2001. Recent progress in the Na translocating NADH-quinone reductase. *Biochimica et Biophysica acta*. 1505: 37-44.

He Q., Huang K.H., He Z., Alm E.J., Fields M.W., Hazen T.C., Arkin A.P., Wall J.D., and Zhou J. 2006. Energetic consequences of nitrite stress in *Desulfovibrio vulgaris* Hildenborough, inferred from global transcriptional analysis. *Applied Environmental Microbiology.* 72: 4370-4381.

Heidelberg, J. F., R. Seshadri, S. A. Haveman, C. L. Hemme, I. T. Paulsen, J. F. Kolonay, J. A. Eisen, N. Ward, B. Methe, L. M. Brinkac, S. C. Daugherty, R. T. Deboy, R. J. Dodson, A. S. Durkin, R. Madupu, W. C. Nelson, S. A. Sullivan, D. Fouts, D. H. Haft, J. Selengut, J. D. Peterson, T. M. Davidsen, N. Zafar, L. W. Zhou, D. Radune, G. Dimitrov, M. Hance, K. Tran, H. Khouri, J. Gill, T.R. Utterback, T.V. Feldbylum, J.D. Wall, G. Voordouw, and C.M. Fraser . 2004. The genome sequence of the anaerobic, sulfate-reducing bacterium *Desulfovibrio vulgaris* Hildenborough. *Nature Biotechnology.* 22: 554-559.

Henstra, A. M., Dijkema, C., and Stams, A. J. M. 2007. *Archaeoglobus fulgidus* couples CO oxidation to sulphate reduction and acetogenesis with transient formate accumulation. *Environ. Microbiol*. 9: 1836–1841.

Jorgensen, B.B. 1977. Bacterial sulphate reduction within reduced microniches of oxidized marine sediments. *Mar. Biol.* 41: 7-17.

Jouanneau, Y., H.S. Jeong, N. Hugo, C. Meyer, and J.C. Willison. Overexpression in *Escherichia coli* of the *rnf* genes from *Rhodobacter capsulatus*. 1998. *European Journal of Biochemistry*. 251: 54-64.

Klonowska, A., Clark, M.E., Thieman, S.B., Giles, B.J., Wall, J.D., and Fields, M.W. 2008. Hexavalent chromium reduction in *Desulfovibrio vulgaris* Hildenborough causes transitory inhibition of sulfate reduction and cell growth. *Applied Microbiology Biotechnology*. 78: 1007-1016.

Laanbroek, H. J., Geerligs, H. J., Sijtsma, L., and Veldkamp, H. 1984. Competition for sulfate and ethanol among *Desulfobacter, Desulfobulbus, and Desulfovibrio* species isolated from intertidal sediments. *Appl. Environ. Microbiol*. 47: 329–334.

Larson, R.A., M.M. Wilson, A.M. Guss, and W.W. Metcalf. 2002. Genetic analysis of pigment biosynthesis in *Xanthobacter autotrophicus* Py2 using a new, highly efficient transposon mutagenesis system that is functional in a wide variety of bacteria. *Archives of Micriobiology.* 178: 193-201.

Li, X., Z. He, and J. Zhou. 2005. Selection of optimal oligonucleotide probes for microarrays using multiple criteria, global alignment and parameter estimation. *Nucleic Acids Research*. 33: 6114-6123.

Lovley, D. R. and Phillips, E. J. 1992. Reduction of uranium by *Desulfovibrio desulfuricans. Appl. Environ. Microbiol*. 58: 850–856.

Lovley, D. R., Roden, E. E., Phillips, E. J. P., and Woodward, J. C. 1993. Enzymatic iron and uranium reduction by sulphate-reducing bacteria. *Mar. Geol*. 113: 41–53.

Lovley, D. R., P. K. Widman, J. C. Woodward, and E. J. P. Phillips. 1993. Reduction of uranium by cytochrome-c_3 of *Desulfovibrio vulgaris*. *Applied & Environmental Microbiology.* 59: 3572-3576.

Lovley, D. R. and Phillips, E. J. 1994. Reduction of chromate by *Desulfovibrio vulgaris* and its c3 cytochrome. *Appl. Environ. Microbiol*. 60: 726–728.

Macy, J.M., Santini, J.M., Pauling, B.V., O'Neill, A.H., and Sly, L.I. 2000. Two new arsenate/sulfate-reducing bacteria: mechanisms of arsenate reduction. *Arch. Microbiol.* 173: 49-57.

Miller, Suzanne M. 2005. Examination of specific amino acid residues of *Desulfovibrio desulfuricans* cytochrome c_3 in electron transfer.

Moore, W.E.C., Johnson, J.L., and Holdeman, L.V. 1976. Emendation of *Bacteroidaceae* and *Butyrivibrio* and descriptions of *Desulfomonas* gen. nov. and ten new species of the genera *Desulfomonas, Butyrivibrio, Eubacterium, Clostridium* and *Ruminococcus*. *Int. J. Syst. Bact.* 26: 238-252.

Morita, Y., K. Kodama, S. Shiota, T. Mine, A. Kataoka, T. Mizushima, and T. Tsuchiya. 1998. NorM, a putative multidrug efflux protein, of *Vibrio parahaemolyticus*. *American Society for Microbiology*. 42: 1778-1782.

Moura, I., Bursakov, S., Costa, C., and Moura, J.J.G. 1997. Nitrate and nitrite utilization in sulfate-reducing bacteria. *Anaerobe*. 3: 279-290.

Mukhopadhyay, A., Z. He, E.J. Alm, A.P. Arkin, E.E. Baidoo, S.C. Borglin, W. Chen, T.C. Hazen, Q. He, H.Y. Holman, K. Huang, R. Huang, D.C. Joyner, N. Katz, M.

Keller, P. Oeller, A. Redding, J. Sun, J. Wall, J. Wei, Z. Yang, H.C. Yen, J. Zhou, and J.D. Keasling. 2006. Salt stress in *Desulfovibrio vulgaris* Hildenborough: an integrated genomics approach. *Journal of Bacteriology*. 188: 4068-4078.

Mukhopadhyay, A., Redding, A.M., Joachimiak, M.P., Arkin, A.P., Borglin, S.E., Dehal, P.S., Chakraborty, R., Geller, J.T., Hazen, T.C., He, Q., Joyner, D.C., Martin, V.J., Wall, J.D., Yang, Z.K., Zhou, J., and Keasling, J.D. 2007. Cell-wide responses to low-oxygen exposure in *Desulfovibrio vulgaris* Hildenborough. *Jouranl of Bacteriology*. 189: 5996-6010.

Nanninga, H.J. and Gottschal, J.C. 1987. Properties of *Desulfovibrio carbinolicus* sp. nov. and other sulfate-reducing bacteria isolated from an anaerobic-purification plant. *Applied and Environmental Microbiology.* 53: 802-809.

Nazina, T. N., Ivanova, A. E., Kanchaveli, L. P., and Rozanova, E. P. 1987. A new sporeforming thermophilic methylotrophic sulphate reducing bacterium, *Desulfotomaculum kuznetsovii* sp. nov. *Mikrobiologiia* 57: 823–827.

Nies, D.H. and Silver, S. 1995. Ion efflux systems involved in bacterial metal resistances. *Journal of Industrial Microbiology*. 14: 186-199.

Nilsen, R. K., Beeder, J., Thostenson, T., and Torsvik, T. 1996. Distribution of thermophilic marine sulfate reducers in North Sea oil field waters and oil reservoirs. *Appl. Environ. Microbiol*. 62: 1793–1798.

Odom, J. M. 1993. Industrial and Environmental Activities of Sulfate-Reducing Bacteria. Pages 159-210 in J. M. S. Odom, R., ed. *The Sulfate-Reducing Bacteria: Contemporary Perspectives*. Springer-Verlag, New York.

Ollivier, B., Cord-Ruwisch, R., Hatchikian, E. C., and Garcia, J.L. 1988. Characterization of *Desulfovibrio fructosovorans* sp. nov. *Arch. Microbiol*. 149: 447–450.

Park, H. S., Lin, S., and Voordouw, G. 2007. Ferric iron reduction by Desulfovibrio vulgaris Hildenborough wild type and energy metabolism mutants. *Antonie van Leeuwenhoek.* 93: 79–85.

Parshina, S. N., Sipma, J., Nakashimada, Y., Henstra, A.M., Smidt, H., Lysenko, A.M., Lens, P.N.L., Lettinga, G., Stams, A.J.M. 2005. *Desulfotomaculum carboxydovorans* sp. nov., a novel sulphate-reducing bacterium capable of growth at 100% CO. *Int. J. Syst. Evol. Microbiol*. 55: 2159–2165.

Pattarkine, M.V., J.J. Tanner, C.A. Bottoms, Y.-H. Lee, and J.D. Wall. 2006. *Desulfovibrio desulfuricans* G20 tetraheme cytochrome structure at 1.5Å and cytochrome interaction with metal complexes. *Journal of Molecular Biology.* 358: 1314-1327.

Payne, R.B., Gentry, D.A., Rapp-Giles, B.J., Casalot, L., and Wall, J.D. 2002. Uranium reduction by *Desulfovibrio desulfuricans* strain G20 and a cytochrome c_3 mutant. *Applied and Environmental Microbiology*. 68: 3129-3132.

Payne, Rayford B. 2005. Energy metabolism and uranium (VI) reduction by *Desulfovibrio*.

Pereira, I.A.C., LeGall, J., Zavier, A.V., and Teixeira, M. 2000. Characterization of heme c nitrite reductase from a non-ammonifying microorganism, *Desulfovibrio vulgaris* Hildenborough. *Biochimica et Biophysica Acta.* 1481: 119-30.

Phadtar, A. 2004. The cold shock response. In *Bacterial Stress Responses*, ed. G. Storz and R. Hengge-Aronis. ASM Press, Washington, D.C., pp. 33-45.

Postgate, J. 1984. *The Sulfate-Reducing Bacteria*. Cambridge University Press, Cambridge.

Rapp, B.J. and J.D. Wall. 1987. Genetic Transfer in Desulfovibrio desulfuricans. *Proceeding of the National Academy of Science U S A.* 9128-9130.

Ravenschlag, K., Sahm, K., Knoblauch, C., Jørgensen, B. B., and Amann, R. 2000. Community structure, cellular rRNA content, and activity of sulfate-reducing bacteria in marine Arctic sediments. *Appl. Environ. Microbiol*. 66: 3592–3602.

Rissati, J. B., Capman, W. C., and Stahl, D. A. 1994. Community structure of a microbial mat: the phylogenetic dimension. *Proc. Natl Acad. Sci. USA*. 91: 10173–10177.

Rodionov, D. A., I. Dubchak, A. Arkin, E. Alm, and M. S. Gelfand. 2004. Reconstruction of regulatory and metabolic pathways in metal-reducing δ-proteobacteria. *Genome Biology*. 5**:** R90.

Saeki, K. and H. Kumagai. 1998. The rnf gene products in *Rhodobacter capsulatus* play an essential role in nitrogen fixation during anaerobic DMSO-dependent growth in the dark. *Archives of Microbiology*. 169: 464-467.

Sasi Jyothsna T.S., Sasikala, C.H., and Ramana C.V. 2008. *Desulfovibrio psychrotolerans* sp. nov., a pschrotolerant and moderately alkaliphilic sulfate reducing deltaproteobacterium from the Himalayas. *International Journal of Systematic and Evolutionary Microbio*. 58: 821-825.

Sass, H., Cypionka, H., and Babenzien, H.-D. 1997. Vertical distribution of sulphate reducing bacteria at the oxic-anoxic interface in sediments of the oligotrophic Lake Stechlin. *FEMS Microbiol. Ecol.* 22: 245-255.

Sass, A., Rutters, H., Cypionka, H., and Sass, H. 2002. *Desulfobulbus mediterraneus* sp. nov., a sulphatereducing bacterium growing on mono- and disaccharides. *Arch. Microbiol.* 177: 468–474.

Schnell, S., Bak, F., and Pfennig, N. 1989. Anaerobic degradation of aniline and dihydroxybenzenes by newly isolated sulfate-reducing bacteria and description of *Desuifobacterium anilini*. *Arch. Microbiol.* 152: 556-563

Schramm, A., Santegoeds, C.M., Nielsen, H.K., Plough, H., Wagner, M., Pribyl, M., Wanner, J., Amann, R., and De Beer, D. 1999. On the occurrence of anoxic microniches, denitrification, and the sulphate reduction in aerated activated sludge. *Applied Environmental Microbiology*. 65: 4189-4196.

Silver, S. 1996. Bacterial resistances to toxic metal ions – a review. *Gene*. 179: 9-19.

Stams, A. J. M., Hansen, T. A., and Skyring, G. W. 1985. Utilization of amino acids as energy substrates by two marine *Desulfovibrio* strains. *FEMS Microbiol. Ecol*. 31: 11–15.

Stams, A. J. M., Oude Elferink, S. J. W. H., and Westermann, P. 2003. Metabolic interactions between methanogenic consortia and anaerobic respiring bacteria. Adv. *Biochem. Eng. Biotechnol*. 81: 31–56.

Steger, J.L., Vincent, C., Ballard, J.D., and Krumholz, L.R. 2002. *Desulfovibrio* sp genes involved in the respiration of sulphate during metabolism of hydrogen and lactate. *Applied Environmental Microbiology*. 68: 1932-1937.

Stoylar, S., Van Dien, S., Hillesland, K.L., Pinel, N., Lie, T.J., Leigh, J.A., and Stahl, D.A. 2007. Metabolic modeling of a mutualistic microbial community. *Molecular Systems Biology*. 3: 92.

Stolyar, S., He Q., Joachimiak, M.P., He, Z., Yang, Z.K., Borglin, S.E., Joyner, D.C., Huang, K., Alm, E., Hazen, T.C., Zhou, J., Wall, J.D., Arkin, A.P., and Stahl, D.A.. 2007. Response of *Desulfovibrio vulgaris* to alkaline stress. *Journal of Bacteriology*. 189: 8944-8952.

Tanimoto, Y. and Bak, F. 1994. Anaerobic degradation of methylmercaptan and dimethyl sulfide by newly isolated thermophilic sulfate-reducing bacteria. *Appl. Environ. Microbiol.* 60: 2450–2455.

Tucker, M. D., Barton, L. L., and Thompson, B. M. 1998. Reduction of Cr, Mo, Se and U by *Desulfovibrio desulfuricans* immobilized in polyacrylamide gels. *J. Ind. Microbiol. Biotechnol*. 20: 13–19.

Vladar, P., Rusznyak, A., Marialigeti, K., and Borsodi, A.K. 2008. Diversity of sulfate reducing bacteria inhabiting the rhizosphere of *Phragmites australis* in Lake Velencei (Hungary) revealed by a combined cultivation-based and molecular approach. *Microb. Ecol.* 56: 64-75.

Von Wolzogen Kuhr, C. A. H., and I. S. van der Vulgt. 1934. The graphitization of cast iron as an electrobiochemical process in anaerobic soils. *Water*: 147-165.

Wall, J.D., Rapp-Giles, B.J., and Rousset, M. 1993. Characterization of a small plasmid from *Desulfovibrio desulfuricans* and its use for shuttle vector construction. J*ournal of Bacteriology.* 175: 4121-4128.

Weimer, P.J., M. J. van Kavelaar, C. B. Michel, and T. K. Ng. 1988. Effect of phosphate on the corrosion of carbon steel and on the composition of the corrosion products in two-stage chemostat cultures of *Desulfovibrio desulfuricans* G100A. *Appl. Environ. Microbiol.* 54: 386-396.

Widdel, F. 1988. *Microbiology and Ecology of Sulfate- and Sulfur-Reducing Bacteria*. Wiley, New York.

Wolfe, B.M., Lui, S.M., and Cowan, J.A. 1994. Desulfoviridin, a multimeric-dissimilatory sulfite reductase from *Desulfovibrio vulgaris* Hildenborough purification, characterization, kinetics and EPR studies. *European Journal of Biochemistry*. 223: 79-89.